https://doi.org/10.1016/j.ejmech.2019.05.062

Elsevier Editorial System(tm) for European Journal of Medicinal Chemistry
Manuscript Draft

Manuscript Number: EJMECH-D-19-00581R1

Title: Investigating 1,2,3,4,5,6-hexahydroazepino[4,3-b]indole as scaffold of butyrylcholinesterase-selective inhibitors with additional neuroprotective activities for Alzheimer's disease

Article Type: Research Paper

Keywords: Alzheimer's disease
Azepino[4,3-b]indole
Acetylcholinesterase
Butyrylcholinesterase
Amyloid-β aggregation
Neuroprotection

Corresponding Author: Dr. Modesto de Candia,

Corresponding Author's Institution: University of Bari

First Author: Rosa Purgatorio, Dr

Order of Authors: Rosa Purgatorio, Dr; Modesto de Candia; Marco Catto, Dr; Antonio Carrieri, Prof; Leonardo Pisani, Dr; Annalisa De Palma, Dr; Maddalena Toma, Dr; Olga A Ivanova, Dr; Leonid G Voskressensky, Prof; Cosimo Damiano Altomare, Prof

Abstract: Due to the role of butyrylcholinesterase (BChE) in acetylcholine hydrolysis in the late stages of the Alzheimer's disease (AD), inhibitors of butyrylcholinesterase (BChE) have been recently envisaged, besides acetylcholinesterase (AChE) inhibitors, as candidates for treating mild-to-moderate AD. Herein, synthesis and AChE/BChE inhibition activity of some twenty derivatives of 1,2,3,4,5,6-hexahydroazepino[4,3-b]indole (HHAI) is reported. Most of the newly synthesized HHAI derivatives achieved the inhibition of both ChE isoforms with IC50s in the micromolar range, with a structure-dependent selectivity toward BChE. Apparently, molecular volume and lipophilicity do increase selectivity toward BChE, and indeed the N2-(4-phenylbutyl) HHAI derivative 15d, which behaves as a mixed-type inhibitor, resulted the most potent (IC50 0.17 □M) and selective (> 100-fold) inhibitor toward either horse serum and human BChE. Moreover, 15d inhibited in vitro self-induced aggregation of neurotoxic amyloid-□ (Aβ) peptide and displayed neuroprotective effects in neuroblastoma SH-SY5Y cell line, significantly recovering ($P < 0.001$) cell viability when impaired by A□1-42 and hydrogen peroxide insults. Overall, this study highlighted HHAI as useful and versatile scaffold for developing new small molecules targeting some enzymes and biochemical pathways involved in the pathogenesis of AD.

Re: Submission revised manuscript EJMECH-D-19-00581

Dear Editor,

We herewith submit the revised version of the manuscript entitled: “Investigating 1,2,3,4,5,6-hexahydroazepino[4,3-*b*]indole as scaffold of butyrylcholinesterase-selective inhibitors with additional neuroprotective activities for Alzheimer's disease” (co-authored by R. Purgatorio, M. de Candia, M. Catto, A. Carrieri, L. Pisani, A. De Palma, M. Toma, O.A. Ivanova, L.G. Voskressensky, and C.D. Altomare).

Answers to the referee’s remarks/comments are reported below.

The following items have been uploaded in the editorial system of EJMECH:

- revised manuscript and figure source file;
- highlights file;
- graphical abstract file;
- supporting information file.

Thank you for your kind consideration and remain
Yours sincerely,

Dr. Modesto de Candia
(Corresponding Author)

e-mail: modesto.decandia@uniba.it
Department of Pharmacy – Drug Sciences, University of Bari “Aldo Moro”
Via E. Orabona 4, I-70125 Bari (Italy)
Phone: +390805443573
Fax: +390805442230

Re: Submission revised manuscript EJMECH-D-19-00581

Dear Editor,

We herewith submit the revised version of the manuscript entitled: "Investigating 1,2,3,4,5,6-hexahydroazepino[4,3-*b*]indole as scaffold of butyrylcholinesterase-selective inhibitors with additional neuroprotective activities for Alzheimer's disease" (co-authored by R. Purgatorio, M. de Candia, M. Catto, A. Carrieri, L. Pisani, A. De Palma, M. Toma, O.A. Ivanova, L.G. Voskressensky, and C.D. Altomare).

Answers to the referee's remarks/comments are reported below.

The following items have been uploaded in the editorial system of EJMECH:

- revised manuscript and figure source file;
- highlights file;
- graphical abstract file;
- supporting information file.

Thank you for your kind consideration and remain
Yours sincerely,

Dr. Modesto de Candia
(Corresponding Author)

e-mail: modesto.decandia@uniba.it
Department of Pharmacy – Drug Sciences, University of Bari "Aldo Moro"
Via E. Orabona 4, I-70125 Bari (Italy)
Phone: +390805443573
Fax: +390805442230

Replies to Referees' suggestions and comments

The changes in the manuscript are highlighted in red.

Reviewer #1:

C: Manuscript titled "Investigating 1,2,3,4,5,6-hexahydroazepino[4,3-*b*]indole as scaffold of butyrylcholinesterase selective inhibitors with additional neuroprotective activities for Alzheimer's disease" is an excellent piece of work related to MTDLs in AD area. It can be accepted in EJMC after carefully addressing all the minor issues raised below.

R: Thanks to the referee for her/his good opinion about the submitted work.

C: ***Minor revisions:***

1) Newhexahydroazepino[4,3-b]indole / New hexahydroazepino[4,3-b]indole Done

2) multipotentanti-Alzheimer agents. / multi-potent anti-Alzheimer's agents Done

3) 15dshowed / 15d showed Done

4) andH2O2-induced / and H2O2-induced Done

5) damagein / damage in Done

C: The following references related to your research must be introduced:

a) Chalupova K et al. Eur J Med Chem. 2019 Apr 15;168:491-514. doi: 10.1016/j.ejmech.2019.02.021. Epub 2019 Feb 27. B) Kaniakova M. et al. Curr Alzheimer Res. 2019 Feb 28. doi: 10.2174/1567205016666190228122218. c) Hepnarova V. et al. Eur J Med Chem. 2018 Apr 25;150:292-306. doi: 10.1016/j.ejmech.2018.02.083. d) Panek D. et al. ACS Chem Neurosci. 2018 May 16;9(5):1074-1094. doi: 10.1021/acschemneuro.7b00461. e) Panek D. et al. Eur J Med Chem. 2017 Jan 5;125:676-695. doi: 10.1016/j.ejmech.2016.09.078.

R: Done

Major revisions:

C: Carefully revise highlights, it contains many typos.

R: Done.

C: There is no correlation between binding ligand energy obtained from in silico that can be extrapolated into in vitro data, thus the sentence "The estimation of free energy variation between 13a and 15d ($\Delta\Delta G$13a/15d = -5.12 ± 0.57 kcal/mole) was in line with the difference observed in the

IC50 values (high-ranked docking poses in Supp. Info.)." is useless and has to be omitted from the text.

R: The sentence has been removed.

Reviewer #2:

The manuscript entitled "Investigating 1,2,3,4,5,6-hexahydroazepino[4,3-b]indole as scaffold of butyrylcholinesterase-selective inhibitors with additional neuroprotective activities for Alzheimer's disease" by Rosa Purgatrio et al. described some novel synthetic compounds with beneficial biological activities against Alzheimer's disease.

By the way, there are some concerns as follow:

C: As the cytotoxicity of Aβ is due to its aggregates, the authors should explain how they examined the entrance and aggregation of Aβ inside cells.

R: Presumably, the cellular events triggered by $A\beta_{42}$ are the same as described in many papers, involving neuronal inflammation, oxidative stress, altered membrane permeability. At this stage of the study, we aimed at screening, through a robust cell model, the cytoprotection exerted by our HHAI compounds against $A\beta_{42}$-induced neuronal toxicity, rather than investigating in detail the underlying cell events. The first sentence in section "2.5.2. Neuroprotective activity against $A\beta_{1\text{-}42}$ and ROS" has been accordingly modified.

C: There are two fig4 in the manuscript that should be corrected.

R: Sorry, it was our mistake! The 'second' Fig. 4 has been changed in Figure 5.

C: In fig 4-1, the compounds showed less activity than quercetin. As shown in fig4 the difference is statistically significant. The authors should discuss more about this difference.

R: Quercetin, as strong in vitro inhibitor of Aβ aggregation, is a widely used positive control in this kind of biophysical assays. The tested HHAI compounds, albeit significantly less active than quercetin, displayed antiaggregating effects of moderate potency. Some comments about the observed differences, likely due to the lack in the HHAI compounds of some essential pharmacophore features for anti-Aβ activity, have been added to complement Section 2.5.1.

C: In fig 4-2, compound **15d** showed some cytotoxicity after 48 h, but there isn't any explanation in the manuscript. The authors should discuss more.

R: Tested alone, **15d** showed some own cytotoxic effects (ca. 30% decrease in cell viability) after 48 h, while maintaining a protecting effect against Aβ-induced toxicity, slightly lower than that observed at 24 h. Within the limits of the cell assay performed, it is not easy to provide a conclusive explanation of the observed time-dependent effect. However, some reasonable arguments, related to possible time-dependent physical and chemical/metabolic stability of compound **15d**, have been introduced and a sentence added to complement section 2.5.2.

Reviewer #3:

C: Introduction is well written with sufficient information for the topic being investigated.

C: Why were the compounds tested at a higher concentration of 100 μM for A<beta> aggregation assay? Ideally concentrations similar to the one used in BChE inhibition study should be employed here. Were there any issues on solubility of the compounds at such high concentration?

R: This is a biophysical test used to preliminarily assess the potential of newly synthesized compounds to inhibit Aβ self-aggregation. In vitro inhibition of $A\beta_{40}$ aggregation is achieved through a medium-throughput screening assay developed in our laboratory (ref. 45), in which the conc. of $A\beta_{40}$ is 30 μM. For the sake of comparability, in the experimental protocol we test compounds at 100 μM, reserving the IC_{50} measurement only to highly active compounds (i.e. those showing > 80% inhibition at 100 μM). Since the test is performed at 10% v/v DMSO concentration, generally there are not solubility issues. In our experience, DMSO can be raised to 20% in the (actually rare) cases of poorly soluble compounds, without affecting reproducibility. In the case of HHAI derivatives tested in this work, any solubility issue was observed.

C: In contrast, for neuroprotective effect, concentration of 5 μM was used. Hence the range of concentration where the compound is active varies from 170 nM (for BChE inhibition) to 100 μM (anti A<beta> aggregation). No doubt the compound (15d) showed multiple mechanisms of action, but how does one translate the different concentrations used in this study into meaningful dose for in vivo studies (in animals and human)?

R: This reviewer's comment evokes a hard issue of the multitarget approach, that is the proper balancing of the different activities and related doses. One may discuss whether this balancing is mandatory or not in the early stage of in vitro screening. Indeed, at this stage, our aim was not finding out a new "drug" but identifying new hits that would be worth investigating through further pharmacological and molecular optimization studies. We think that with the HHAI derivatives described herein there should be wide margin for ameliorating the overall activity profile. In this

light, the imbalance of several activities will be carefully investigated in vivo, provided that the active doses may be different, and differently dependent for each target from ADME properties.

C: There are 2 figures labelled as Figure 4.

R: Sorry for the mistake. The figures have been differently labeled as Figures 4 and 5.

C: Figure 4 (sec 2.5.1) - The results indicated that the anti A<beta> aggregation activity of the compounds was significantly lower than quercetin. Hence, how does one classify the potency of the compound? Are they considered to have weak or moderate activity?

R: The tested HHAI compounds, albeit significantly less active than quercetin, displayed antiaggregating effects of moderate potency. Some comments about the observed differences, likely due to the lack in the HHAI compounds of some essential structural features for anti-Aβ activity, have been added to complement Section 2.5.1.

C: Figure 4 (sec 2.5.2) - It was mentioned in the text that compound 15d did not show any cytotoxicity, however at 48h, there was significant reduction in cell viability of about 30% in 15d group (tested alone) as compared to untreated cells. Isn't that considered cytotoxicity?

R: The referee is right! For unexplained reasons, in the first manuscript we did not highlight what it's clear from the bar plot in the 'old' Fig. 4 (now Fig. 5). Tested alone, **15d** showed some own cytotoxic effects (ca. 30% decrease in cell viability) after 48 h, while maintaining a protecting effect against Aβ-induced toxicity, slightly lower than that observed at 24 h. Some reasonable arguments, related to possible time-dependent physical and chemical/metabolic stability of compound **15d**, have been introduced and a sentence added to complement section 2.5.2.

C: For hydrogen peroxide model, few concentrations ranging from 1-100 μM were used. What is the rationale of selecting the range of concentrations? If 15d showed potential cytotoxicity at 5 μM at 48h, are there any cytotoxicity expected at higher concentration?

R: In this assay, the concentration range is usually kept wide, in order to determine the antioxidant potency more accurately. There is no relationship with the neuroprotection assay from amyloid insult. The DCFH test does not evaluate cell viability, but antioxidant activity of test compound as scavenger of ROS produced by H_2O_2 insult. The DCFH test was carried out in few hours, and it is based on enzymatic conversion of DCFH to the polar DCF by hydrolysis, which is possible only in viable cells.

C: Sec 4.8 - For A<beta> study, the compound was diluted with A<beta> solution before added into the cells. Will there be any physical interaction between the two that may reduce the amount of A<beta> available to cause stress to the cells?

R: The biochemical insult induced by Aβ is related to the formation of soluble oligomers of aggregating protein. The mechanism of inhibition of oligomerization is amenable to a physical interaction of inhibitor with Aβ monomers and/or early oligomers. In any case, sequestering of low molecular weight Aβ species is a valuable strategy to avoid cellular damage.

C: English language editing is required for this manuscript as there are many long-winded sentences, e.g. the first sentence of the abstract.

R: English language has been revised.

Reviewer #4:

C: In this manuscript synthesis and AChE/BChE inhibition activity of twenty derivatives of 1,2,3,4,5,6-hexahydroazepino[4,3-*b*]indole (HHAI) is reported. Most of the newly synthesized HHAI derivatives achieved the inhibition of both ChE isoforms with IC50s in the micromolar range, with a structure-dependent selectivity toward BChE.

C: Overall well documented manuscript but literature and introduction should be supported by most recent reported Anti-Alzheimer agents like Bioorganic & medicinal chemistry 24 (10), 2352-2359, European journal of medicinal chemistry 155, 49-60, Chemical biology & drug design 88 (6), 889-898, Chemical Biology & Drug Design 92 (5), 1859-1866 and European Journal of Medicinal Chemistry 152, 600-614.

R: Done.

C: (IC_{50}) values of eeAChE and hsBChE for all compounds can be included in one table if possible.

R: In our opinion, the breakdown in different tables can help the reader to grasp the most of the structure-activity relationships.

Reviewer #5:

The manuscript entitled Investigating 1,2,3,4,5,6-hexahydroazepino[4,3-b]indole as scaffold of butyrylcholinesterase-selective inhibitors with additional neuroprotective activities for Alzheimer's disease needed major revisions to become acceptable for publication in Eur. J. Med. Chem.

C: Why the authors prepare compounds in hydrochloride salts? Is there any try to separate them as the free base forms?

R: Final tested derivatives were prepared as hydrochloride salts, due to its better aqueous solubility, and easy purification by crystallization.

C: C-NMR, HRMS are necessary for all new compounds.

R: ^{13}C-NMR spectra of all the newly synthesized compounds have been reported in experimental section of manuscript. The data reported as "ESI-MS m/z calcd for CxHyNz $[M+H]^+$…., found …." refer to HRMS data; we modified "ESI-MS" as "HRMS".

C: The rational design is not interesting in my opinion and should be improved. The synthesized compounds are not reasonable in terms of medicinal chemistry. Different groups at different positions are needed in this case.

R: The present work follows the previous publications of the same groups, about biological investigation of middle-terms heterocycles fused on pyrrole/indole. We recently reported multitarget activity of the 2,3,4,5-tetrahydroazepino[4,3-*b*]indole(1*H*)-2-one derivatives (THAI). Unfortunately, these compounds suffered in most cases of low aqueous solubility. As also mentioned in this manuscript, the N^2-methylation of compound **6** proved to be detrimental. However, reduction of **6** to the corresponding hexahydro-azepinoindole (HHAI) did retain weak BChE inhibition and potential multitarget activity. Therefore, in this paper we reported a SAR investigation about the suitability of the more soluble HHIA scaffold.

The design description in the introductory section has been modified as follows: "Unfortunately, the lactam derivative **6** suffered from low aqueous solubility, whereas its reduction to the more soluble amino derivative did decrease BChE inhibition potency and increase toxicity toward neuronal cells. Herein, with the aim of better characterizing the azepino[4,3-*b*]indole nucleus as a template for novel MTDLs for treating AD, about twenty N^2-substituted 1,2,3,4,5,6-hexahydroazepino[4,3-b]indole (HHAI) derivatives were synthesized and tested as AChE/BChE inhibitors. The most active ChE inhibitors were then evaluated as Aβ-antiaggregating agent and neuroprotectant against Aβ and oxidative stress insults in neuroblastoma cell line (SH-SY5Y)."

C: The manuscript should be revised by a native speaker.

R: English language has been revised, and grammar and syntax errors eliminated as much as possible.

C: I recommend the authors to investigate the binding mode of active compound to AChE.

R: The binding mode in AChE active site of **15d** had been already investigated but not reported in the first submission. In the revised manuscript the following sentence has been introduced: "The same docking calculation protocol was applied to simulate the binding mode of 15d to *hu*AChE. The observed selectivity was substantially justified by docking results (see Supp. Info.), which showed lower stabilizing interactions with Trp286 in *hu*AChE. The figure with docking pose has been added in the Supplementary Information file."

Investigating 1,2,3,4,5,6-hexahydroazepino[4,3-*b*]indole as scaffold of butyrylcholinesterase-selective inhibitors with additional neuroprotective activities for Alzheimer's disease

Rosa Purgatorio,[a] Modesto de Candia,[a] Marco Catto,[a] Antonio Carrieri,[a] Leonardo Pisani,[a] Annalisa De Palma,[b] Maddalena Toma,[a] Olga A. Ivanova,[c] Leonid G. Voskressensky,[d] and Cosimo D. Altomare[a]*

[a]Department of Pharmacy-Drug Sciences, University of Bari Aldo Moro, Via E. Orabona 4, 70125 Bari, Italy. [b]Department of Biosciences, Biotechnologies and Biopharmaceutics, University of Bari Aldo Moro, Via E. Orabona 4, 70125 Bari, Italy. [c]Department of Chemistry, M. V. Lomonosov Moscow State University, Leninskie Gory 1-3, Moscow 119991, Russian Federation. [d]Organic Chemistry Department, RUDN University, Miklukho-Maklai St, 6, Moscow 117198, Russian Federation.

Graphical abstract

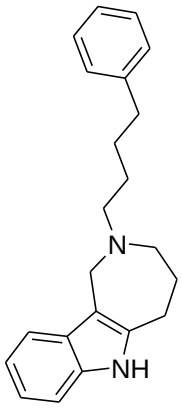

15d

IC_{50} (*h*BChE) = **170 nM**

IC_{50} (*h*AChE) = 20.0 μM

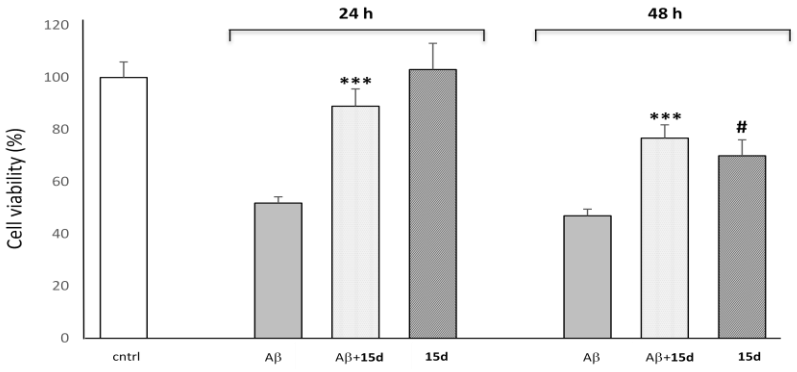

SH-SY5Y cells cytoprotection of **15d** (5 μM) after treatment with $A\beta_{1-42}$(5 μM).

Investigating 1,2,3,4,5,6-hexahydroazepino[4,3-*b*]indole as scaffold of butyrylcholinesterase-selective inhibitors with additional neuroprotective activities for Alzheimer's disease

Rosa Purgatorio,[a] Modesto de Candia,[a] Marco Catto,[a] Antonio Carrieri,[a] Leonardo Pisani,[a] Annalisa De Palma,[b] Maddalena Toma,[a] Olga A. Ivanova,[c] Leonid G. Voskressensky,[d] and Cosimo D. Altomare[a]*

[a]Department of Pharmacy-Drug Sciences, University of Bari Aldo Moro, Via E. Orabona 4, 70125 Bari, Italy. [b]Department of Biosciences, Biotechnologies and Biopharmaceutics, University of Bari Aldo Moro, Via E. Orabona 4, 70125 Bari, Italy. [c]Department of Chemistry, M. V. Lomonosov Moscow State University, Leninskie Gory 1-3, Moscow 119991, Russian Federation. [d]Organic Chemistry Department, RUDN University, Miklukho-Maklai St, 6, Moscow 117198, Russian Federation.

Highlights

- New hexahydroazepino[4,3-*b*]indole derivatives were designed and synthesized as multi-potent anti-Alzheimer's agents.
- Compound **15d** proved to be a potent BChE-selective inhibitor (IC_{50} = 170nM).
- Structure-activity relationships revealed key molecular features for BChE inhibitory potency and selectivity.
- At low micromolar concentrations, **15d** showed protective significant effects ($P < 0.001$) against Aβ- and H_2O_2-induced cell damage in SH-SY5Y neuronal cells.

Investigating 1,2,3,4,5,6-hexahydroazepino[4,3-*b*]indole as scaffold of butyrylcholinesterase-selective inhibitors with additional neuroprotective activities for Alzheimer's disease

Rosa Purgatorio,[a] *Modesto de Candia,*[a]* *Marco Catto,*[a] *Antonio Carrieri,*[a] *Leonardo Pisani,*[a] *Annalisa De Palma,*[b] *Maddalena Toma,*[a] *Olga A. Ivanova,*[c] *Leonid G. Voskressensky,*[d] *and Cosimo D. Altomare*[a]

[a]Department of Pharmacy-Drug Sciences, University of Bari Aldo Moro, Via E. Orabona 4, 70125 Bari, Italy. [b]Department of Biosciences, Biotechnologies and Biopharmaceutics, University of Bari Aldo Moro, Via E. Orabona 4, 70125 Bari, Italy. [c]Department of Chemistry, M. V. Lomonosov Moscow State University, Leninskie Gory 1-3, Moscow 119991, Russian Federation. [d]Organic Chemistry Department, RUDN University, Miklukho-Maklai St, 6, Moscow 117198, Russian Federation.

Author Contributions:

M.d.C., R.P., L.P., O.I.A. and L.G.V. contributed to chemistry and physicochemical data. M.d.C. and R.P. performed enzymes' inhibition measurements. M.C., A.D. and M.T. carried out cell assays and analyzed the biological data analysis. A.C. performed the molecular modeling study. M.d.C. designed the research project, interpreted the SARs and wrote the manuscript. C.D.A. supervised the project and revised the manuscript. All the authors approved the final version of the manuscript.

*Corresponding Author: Phone +39-080-5443573; fax +39-080-5442230; e-mail modesto.decandia@uniba.it

ABSTRACT

Due to the role of butyrylcholinesterase (BChE) in acetylcholine hydrolysis in the late stages of the Alzheimer's disease (AD), inhibitors of butyrylcholinesterase (BChE) have been recently envisaged, besides acetylcholinesterase (AChE) inhibitors, as candidates for treating mild-to-moderate AD. Herein, synthesis and AChE/BChE inhibition activity of some twenty derivatives of 1,2,3,4,5,6-hexahydroazepino[4,3-*b*]indole (HHAI) is reported. Most of the newly synthesized HHAI derivatives achieved the inhibition of both ChE isoforms with IC_{50}s in the micromolar range, with a structure-dependent selectivity toward BChE. Apparently, molecular volume and lipophilicity do increase selectivity toward BChE, and indeed the N^2-(4-phenylbutyl) HHAI derivative **15d**, which behaves as a mixed-type inhibitor, resulted the most potent (IC_{50} 0.17 μM) and selective (> 100-fold) inhibitor toward either horse serum and human BChE. Moreover, **15d** inhibited in vitro self-induced aggregation of neurotoxic amyloid-β (Aβ) peptide and displayed neuroprotective effects in neuroblastoma SH-SY5Y cell line, significantly recovering ($P < 0.001$) cell viability when impaired by $Aβ_{1-42}$ and hydrogen peroxide insults. Overall, this study highlighted HHAI as useful and versatile scaffold for developing new small molecules targeting some enzymes and biochemical pathways involved in the pathogenesis of AD.

Keywords:

Alzheimer's disease

Azepino[4,3-*b*]indole

Acetylcholinesterase

Butyrylcholinesterase

Amyloid-β aggregation

Neuroprotection

Abbreviations

AD, Alzheimer Disease; ACh, Acetylcholine; AChE, Acetylcholinesterase; BChE, Butyrylcholinesterase; CAS, Catalytic anionic site; CNS, Central Nervous System; DCM, dichloromethane; PAS, Peripheral anionic site; PB, Phosphate Buffer; PBS, Phosphate Buffered Saline; SAR, Structure-activity relationship; SH-SY5Y, human neuroblastoma cell line; TBAB, Tetrabutyl ammonium bromide.

1. Introduction

Alzheimer's disease (AD) is the prevailing neurodegenerative and devastating disorder, which accounts for most elderly-related dementias. As summarized in World Alzheimer Report 2018 [1], people affected by AD has been estimated to increase to more than 131 million up to 2050. The histopathological hallmarks of AD are deposition of extracellular neurotoxic amyloid-β (Aβ) peptide aggregates that, with intracellular neurofibrillary tangles of hyperphosphorylated τ-protein, generates senile plaques, by triggering oxidative stress, perturbation of cellular metabolism, and finally synaptic and neuronal loss. In addition, a lower level of the neurotransmitter acetylcholine (ACh) into hippocampus, and progressively into the whole brain cortex, typically contributes to the AD-related cognitive and memory impairment and decline [2,3].

Despite the efforts (and financial resources employed as well) aimed at identifying disease-modifying molecules, only few drugs have been approved for the symptomatic treatment of mild-to-moderate AD (Chart 1), which include the acetylcholinesterase (AChE) inhibitors rivastigmine (**1**), galantamine (**2**), and donepezil (**3**), and the *N*-methyl-D-aspartate receptor (NMDAR) antagonist memantine (**4**). Galantamine (**2**) and donepezil (**3**) are reversible ChE inhibitors, whereas rivastigmine (**1**) is a pseudo-irreversible inhibitor that transfers a carbamate moiety to the catalytic serine residue (followed by slow hydrolysis) in the active sites of both AChE and butyrylcholinesterase (BChE). Regarding memantine (**4**), it has been established that AD patients may further benefit from reduction of NMDAR glutamate-induced Ca^{2+}-mediated excitotoxicity [4].

ACh is mainly hydrolyzed by AChE in the synaptic cleft of the cholinergic neurons, but at higher concentrations it could be also hydrolyzed by BChE, an α-glycoprotein produced in liver and primarily distributed in plasma but also detected in central and peripheral nervous systems. Plasma BChE may be likely responsible for detoxification of xenobiotics [5], whereas BChE expressed and secreted in CNS glial cells and neurons likely acts therein as a co-regulator of cholinergic neurotransmission [6].

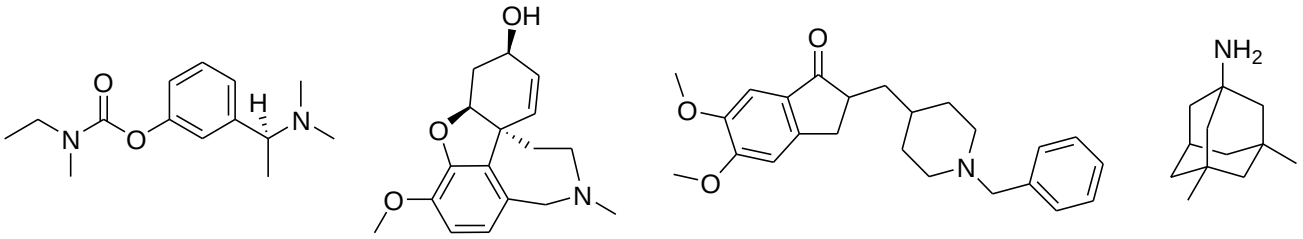

Rivastigmine (**1**) Galantamine (**2**) Donepezil (**3**) Memantine (**4**)

Chart 1. Currently available drugs for the management of AD.

In healthy brain AChE is the main enzyme responsible for ACh regulation, whereas in brain areas of AD patients, a decline of AChE level and a significant increase (30-60%) of BChE expression and activity have been observed [7-9]. Overall, this evidence suggests a role of BChE in AD progression, and then the importance of developing inhibitors targeting BChE, endowed with other neuroprotective activities, as useful drugs for treating AD [10,11].

AChE and BChE share about 70% of structural homology but differ in their three-dimensional structures. AChE contains a 20 Å deep and narrow gorge, and five regions are involved in the ligand binding: (i) the catalytic triad residues (Ser203, His447, Glu334, human species numbering); (ii) the 'oxyanion hole' inside the active center, that stabilizes the transient tetrahedral enzyme-substrate complex; (iii) the 'anionic site' (AS), where Trp86 (conserved in both ChEs) is involved in the orientation and stabilization of trimethylammonium head of ACh, through cation-π interactions; (iv) the 'acyl pocket' interacting with the substrate acyl group; (v) the 'peripheral anionic site' (PAS), located on the rim of the active site gorge [12]. The main differences between AChE and BChE occur in the 'acyl pocket' and PAS, where two Phe residues (Phe295, Phe297) in the AChE 'acyl pocket', which prevent the access of bulkier molecules to the catalytic site, are replaced by two aliphatic residues (Leu286, Val288) in BChE. Furthermore, six out of the fourteen aromatic residues lining the AChE gorge rim and PAS are replaced by aliphatic residues in BChE. Consequently, the BChE cavity is about 200 $Å^3$ larger than the AChE gorge [13-15].

Besides their catalytic function, both enzymes exhibit several noncholinergic (nonenzymatic) functions, related in AD physiopathology. Indeed, both enzymes proved to be involved in processes leading to formation and deposition of Aβ fibrils [16-18]. The peripheral site of AChE interacts with Aβ protein, by enhancing its deposition and aggregation. In contrast, limited knowledge has been reported on mechanism linking amyloidogenesis and BChE, even if a putative role has been associated to plaques formation and maturation. Indeed, BChE was found to be colocalized with Aβ into the senile plaques [7], and selective BChE inhibitors, such as N^1-phenetylnorcymserine (**5**, Chart 2) [6,19-21], proved to reduce fibrils deposition in some cerebral areas (amygdala, hippocampal structures, thalamus and basal ganglia), and ameliorate cognitive dysfunction induced by $A\beta_{40}$ peptide in animal models of AD, likely through a BChE involvement in glia-mediated neuroinflammation associated to AD [22,23].

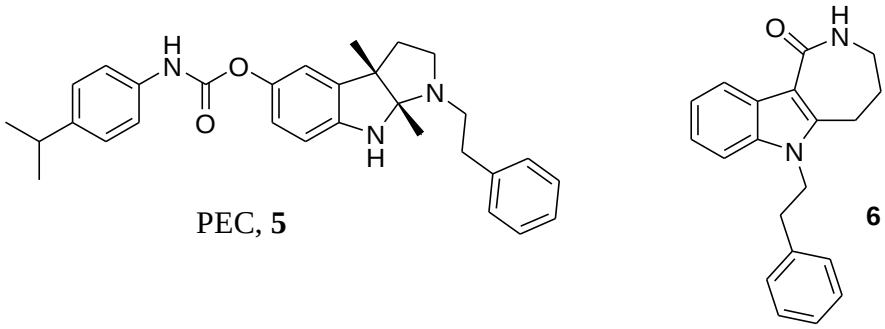

PEC, **5** **6**

Chart 2. Structures of BChE-selective inhibitors.

Selective BChE inhibitors usually contain polycyclic structures [24-27], such as compound **5**, ethopropazine [28,29], quinazolinimine-based derivatives [30,31], carbazole and indolpiperidines [32,33]. Previously, some of us reported efficient syntheses of partially hydrogenated pyrrole- and indole-fused azaheterocycles with six-to-eight-membered ring size [34-36], as scaffolds of novel bioactive compounds, such as antiplatelet [37,38], antimicrobial [39], antioxidant agents [40,41] and AChE inhibitors [42-44]. More recently, some N^6-substituted partially hydrogenated azepino[4,3-*b*]indole derivatives showed selective inhibition of BChE [45]. Azepino-indoles could

be considered homologues of carbazoles and carbolines, exploited as binder moieties in a number of dual-site AChE inhibitors, and multitarget-directed ligands (MTDL) addressing the pathogenic pathways underlying AD. In particular, the 2,3,4,5-tetrahydroazepino[4,3-*b*]indole(1*H*)-2-one derivative **6** (Chart 2) exhibited nanomolar and selective BChE inhibition (IC_{50}s *vs* AChE and BChE 20 and 0.020 μM, respectively), and showed protective activity against NMDA-induced excitotoxicity in neuronal cell line (SH-SY5Y), higher than the NMDAR antagonist memantine **4** [45]. Unfortunately, the lactam derivative **6** suffered from low aqueous solubility, whereas its reduction to the more soluble amino derivative did decrease BChE inhibition potency and increase toxicity toward neuronal cells. Herein, with the aim of better characterizing the azepino[4,3-*b*]indole nucleus as a template for novel MTDLs for treating AD, about twenty N^2-substituted 1,2,3,4,5,6-hexahydroazepino[4,3-*b*]indole (HHAI) derivatives were synthesized and tested as AChE/BChE inhibitors. The most active ChE inhibitors were then evaluated as Aβ-antiaggregating agent and neuroprotectant against Aβ and oxidative stress insults in neuroblastoma cell line (SH-SY5Y).

2. Results and discussion

2.1. Chemistry

Compounds **8a-c**, **12a-b**, and **13b-c** were previously published or prepared using known procedures [46-48], according to Scheme 1. The HHAI compounds **8a-c** were prepared by reduction of respective lactam derivatives **7a-c** [45,47] with $LiAlH_4$ in refluxing 1,4-dioxane. The azepine intermediates **8a-c** were treated with formaldehyde, and the *N*-formyl were catalytically reduced to yield the *N*-methyl derivatives **12a-b** [48]. Compounds **8a-c**, reacted with suitable benzoyl- or phenylalkanoyl chlorides, leading to compounds **9-11**. A reduction reaction, followed by crystallization of the HHAIs as hydrochloride salts, led to **13a-h**, **15a** and **15c-d** in satisfactory yields. For preparing the N^6-methyl derivative **15b**, the phenylacetyl amide **9e** underwent reaction

with MeI and TBAB in a biphasic mixture (1:1 v/v of DCM/25% NaOH) to yield **14a**, which was in turn reduced to **15b** with $LiAlH_4$.

Scheme 1.[a]

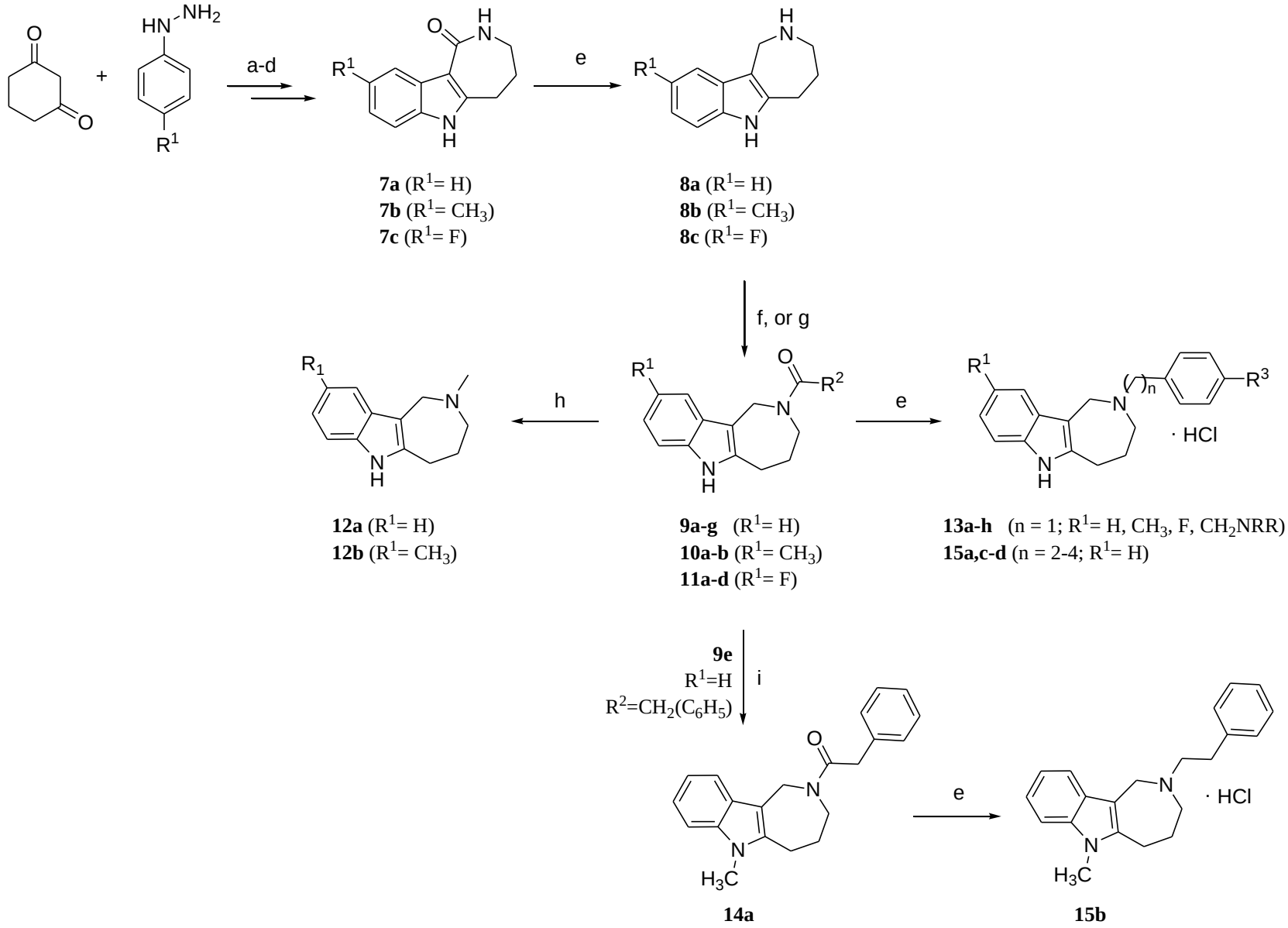

7a (R^1= H)
7b (R^1= CH_3)
7c (R^1= F)

8a (R^1= H)
8b (R^1= CH_3)
8c (R^1= F)

12a (R^1= H)
12b (R^1= CH_3)

9a-g (R^1= H)
10a-b (R^1= CH_3)
11a-d (R^1= F)

13a-h (n = 1; R^1= H, CH_3, F, CH_2NRR)
15a,c-d (n = 2-4; R^1= H)

9e
R^1=H
R^2=$CH_2(C_6H_5)$

14a

15b

[a] Reagents and conditions: a) Water, r.t., overnight, 85%; b) TFA, reflux, 24 h, 65-70%; c) NH_2OH×HCl, AcONa, EtOH/H_2O 2/1 v/v, reflux, 24h, 85-90%; d) 110 °C-preheated PPA, 30 min, 70%; e) 1. $LiAlH_4$, dry dioxane, reflux (50-75%); 2. HCl sat. MeOH solution; f) HCHO, EtOH/H_2O; g) acyl halides, TEA, dry CH_2Cl_2, overnight; h) H_2, PtO_2, EtOH; i) CH_3I, TBAB, 25% NaOH/DCM 1/1 v/v, r.t., 48 h, 55%.

2.2. Inhibition of cholinesterases

The *in vitro* inhibitory activity of the investigated compounds toward electric eel (*ee*) AChE and horse serum (*hs*) BChE were determined by the Ellman colorimetric assay [49]. The half maximal inhibitory concentration values (IC_{50}) are summarized in Tables 1-3 (galantamine **2** and donepezil **3** used as the positive controls).

Table 1. Half maximal inhibitory concentration (IC_{50}) values of *ee*AChE and *hs*BChE of HHAI derivatives **8a-c** and **12a**,**b**.

Cmpd		**R[1]**	**IC_{50} (μM)[a]**	
			***ee*AChE**	***hs*BChE**
8a	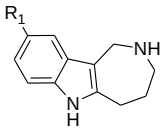	H	70.0 ± 5.0	20 ± 3
8b		CH_3	45.0 ± 2.5	8.0 ± 2.1
8c		F	16.0 ± 1.4	4.3 ± 1.2
12a	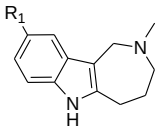	H	7.1 ± 1.7	25.0 ± 2.0
12b		CH_3	25.0 ± 3.0	7.1 ± 0.3
Galantamine, **2**			0.56 ± 0.10	12.0 ± 0.30
Donepezil, **3**			0.021 ± 0.002	2.3 ± 0.12

[a]Seven different concentrations were tested for determining IC_{50} values by regression of the sigmoid dose-response curves through GraphPad Prism software (vers. 5.01); data are means ± SEM of at least three independent measurements.

Compounds **8a-c** and **12a-b** (Table 1) proved to be inhibitors of both ChEs with a potency in the micromolar range. No HHAI derivative resulted in vitro more potent than the standard references **2** and **3** toward AChE. Except for the N^2-Me derivative **12a**, all these compounds showed a preference toward BChE, with inhibition potencies in the low micromolar range.

A net increase of ChEs' inhibition activity was achieved by introducing benzyl groups on the azepine nitrogen (Table 2). The effect of N^2-benzyl groups, also bearing substituents exerting

opposite electronic effects, were stronger on BChE than on AChE inhibition. Higher inhibitory activity and ten-fold BChE selectivity ratio was attained by **13d** (R^3 = 4'-CH_3) and **13e** (R^3 = 4'-F).

Table 2. IC_{50} values of *ee*AChE and *hs*BChE of N^2-benzyl HHAI derivatives **13a-h**.

Cmpd		R^1	R^3	IC_{50} (μM)[b]	
				***ee*AChE**	***hs*BChE**
13a		H	H	8.70 ± 0.40	2.00 ± 0.30
13b		CH_3	H	6.95 ± 1.30	1.20 ± 1.30
13c		F	H	4.96 ± 1.20	2.13 ± 0.20
13d	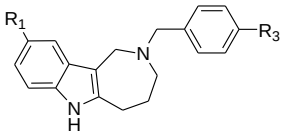	H	4'-CH_3	10.0 ± 2.0	0.95 ± 0.10
13e		H	4'-F	12.0 ± 2.1	1.20 ± 0.20
13f		F	4'-F	4.10 ± 0.70	2.90 ± 1.00
13g		F	4'-CH_2NEt_2	4.80 ± 1.60	1.40 ± 0.60
13h		F	4'-$CH_2N(CH_2)_4$	7.90 ± 1.10	4.30 ± 1.20

[a]See footnote in Table 1; galantamine (**2**) and donepezil (**3**) as positive controls.

In contrast with the 9-methyl derivative (**13b**), the insertion of fluorine on C-9 (**13c**, BChE IC_{50} 2.13 μM) did not improve BChE inhibition potency, whereas diminished the selectivity ratio (**13c** vs **13a**). Among the 9-F congeners, the replacement of 4'-F (**13f**) with the basic 4'-*N,N'*-diethylamino-methyl group (**13g**) did slightly increase the BChE (and not AChE) inhibition potency. This might be due to similar withdrawing effect exerted by fluorine and *N,N'*-diethylamino-methyl group protonated at physiological pH, even if the volume and lipophilicity of alkylamino group seems to play a role, as accounted for the lower activity of the pyrrolidine-methyl congener **13h**.

A SAR comparison (Table 3) of **13c** with the N-benzoyl analog (**11a**) and the previously reported [3,4-*b*] fusion isomer **16** [35] suggests that azepine basic nitrogen and [4,3-*b*] fusion should be preferred features for ChEs' inhibition.

Table 3. Cholinesterases' inhibition IC_{50}s for SAR comparison of **13c** with **11a** and **16**.

IC_{50} (μM)	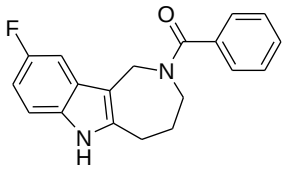	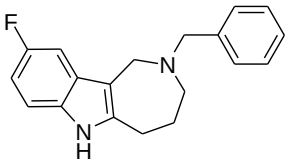	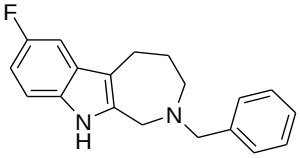
	11a	**13c**	**16**
***ee*AChE**	10.6 ± 1.20	4.96 ± 1.20	10.7 ± 1.10
***hs*BChE**	6.00 ± 1.20	2.13 ± 0.20	3.40 ± 1.40

The effect on ChEs' inhibition potency of the length of alkyl chain in N^2-phenylalkyl HHAI derivatives, as expressed as the number of CH_2 units (*n*), was finally explored (Table 4).

Table 4. Half maximal inhibitory concentration (IC_{50}) values of *ee*AChE and *hs*BChE by N^2-phenylalkyl HHAI derivatives **13a** and **15a-d** ($R^1 = R^3 = H$).

Cmpd		***n***	**IC_{50} (μM)**[a]	
			***ee*AChE**	***hs*BChE**
13a		1	8.7 ± 0.4	2.00 ± 0.3
15a	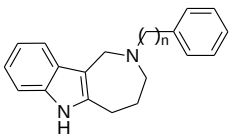	2	9.00 ± 1.5	0.70 ± 0.2
15b[b]		2	12.0 ± 1.9	0.86 ± 0.10
15c		3	20.0 ± 2.1	0.28 ± 0.05
15d		4	20.0 ± 1.8	0.17 ± 0.02

[a]See footnote in Table 1; galantamine (**2**) and donepezil (**3**) as positive controls. [b]N^6-methyl derivative.

The AChE inhibition activity remained unchanged (n = 1, 2) or decreased (n = 3, 4), whereas BChE inhibition enhanced by increasing the alkyl chain length till 3-4 CH_2 units. The methylation of the indole nitrogen in **15b** did not significantly affect ChE inhibition (IC_{50}s close to those of **15a**). Fig. 1 shows the effect of the linker elongation on the BChE/AChE selectivity ratio.

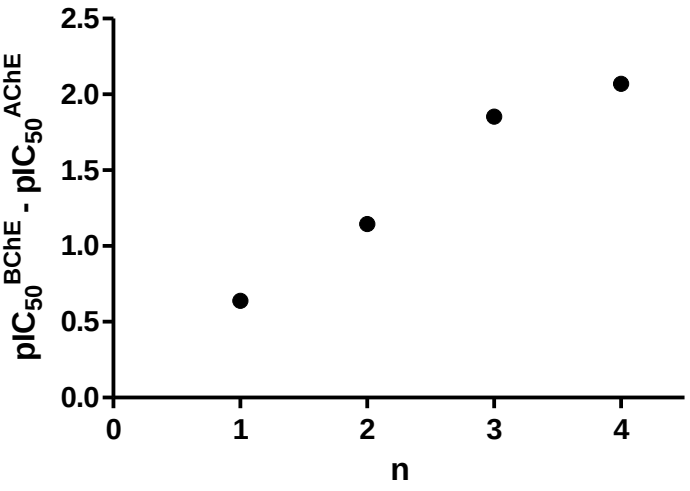

Figure 1. BChE selectivity ratios of N^2-phenylalkyl HHAI derivatives, expressed in log units, as a function of the number of CH_2 units (n) in the alkyl chain.

The mechanism of the BChE inhibition of the most potent *hs*BChE inhibitor **15d** was studied. The Lineweaver-Burk curves were outlined using a fixed amount of BChE and varying concentrations of the substrates between 25 and 300 μM, in the absence or presence of inhibitor at different concentrations (0.1-0.5 μM). Binding of **15d** to BChE changed both V_{max} and K_m values, a trend that is generally ascribed to mixed-type inhibition (Fig. 2). A replot of the slopes versus the corresponding inhibitor concentrations provided a K_i value of 0.098 μM.

The inhibitory activity of **15d** was also evaluated against human (*hu*) ChEs, which share > 80% homology with *ee*AChE and *hs*BChE (Table 4), and any noteworthy species-dependent ChEs' inhibition activity was observed.

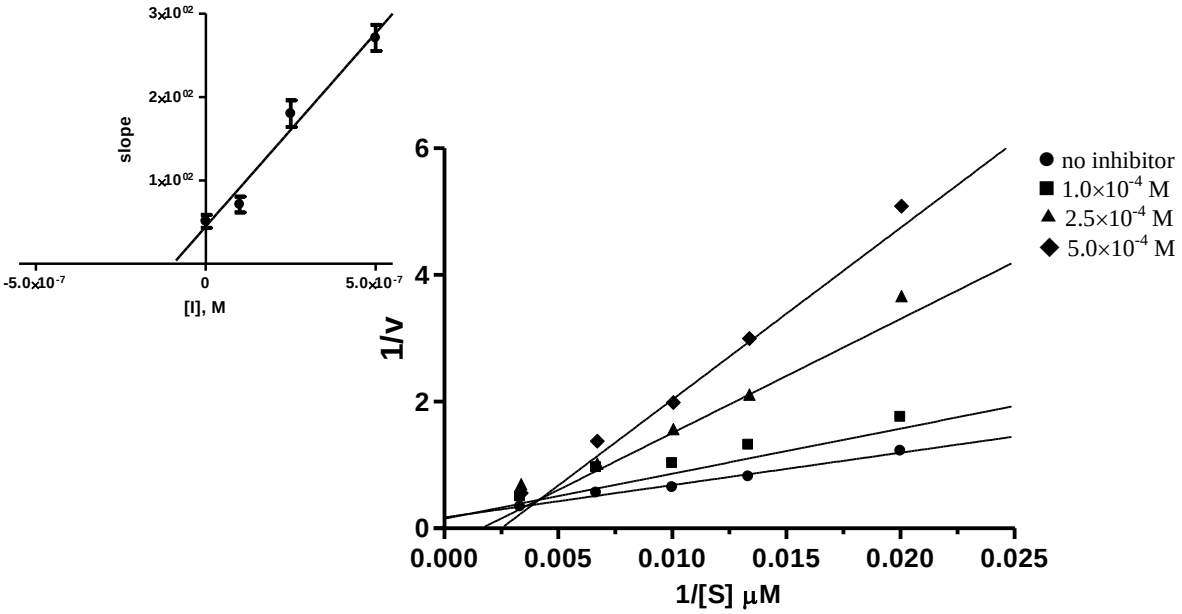

Figure 2. Inhibition kinetics of **15d** using Lineweaver–Burk plots ($r^2 \geq 0.975$) with *hs*BChE (0.18 U/mL) and different substrate (butyrylthiocholine iodide) concentrations (50-300 μM); replot ($r^2 \geq 0.978$) of the slopes versus [I] to determine K_i (0.098 μM) as the *x*-axis intercept is shown in the upper left insert.

Table 4. IC_{50} values of the most potent derivative **15d** against human AChE and BChE.

	IC_{50} (μM)	
	***hu*AChE**	***hu*BChE**
15d	20.0	0.199 ± 0.01
Donepezil	0.016 ± 0.002	4.80 ± 0.50

2.3 Molecular modeling

The binding mode of compound **15d** to *hu*BChE was investigated by molecular docking simulation. As shown in Fig. 3, the whole molecular bundle is merged into the deeper gorge of the BChE active site, with a largely extended ligand-enzyme contact surface (717.52 $Å^2$). The HHAI moiety is oriented towards the top of the choline-binding site via a parallel π-stacking engaging the indole moiety of the ligand and the aromatic side chain of Trp82, whereas the pending 4-phenylbutyl group is laying on the bottom of the acyl-binding pocket through an edge-to-face π-stacking with

Trp231 side chain. The lack or greater weakness of the aromatic interaction of the N^2-benzyl derivative **13a** may explain, at least in part, its lower inhibitory potency with respect to **15d** toward *hu*BChE, as also supported by Free Energy Perturbation (FEP) calculation (see Supp. Info). In addition, two hydrogen bonds further stabilize the ligand-enzyme complex; the first between the positively charged N-2 of **15d** (with assistance of a water molecule) and the Oγ of Thr120, and the second one between the indole NH and C=O of His438 in the backbone. It is worth noting that the highest-scored docking pose of **15d** resembles, regarding the location HHAI moiety, that observed in the X-ray complex of tacrine with BChE (pdb code: 4BDS; Supp. Info.).

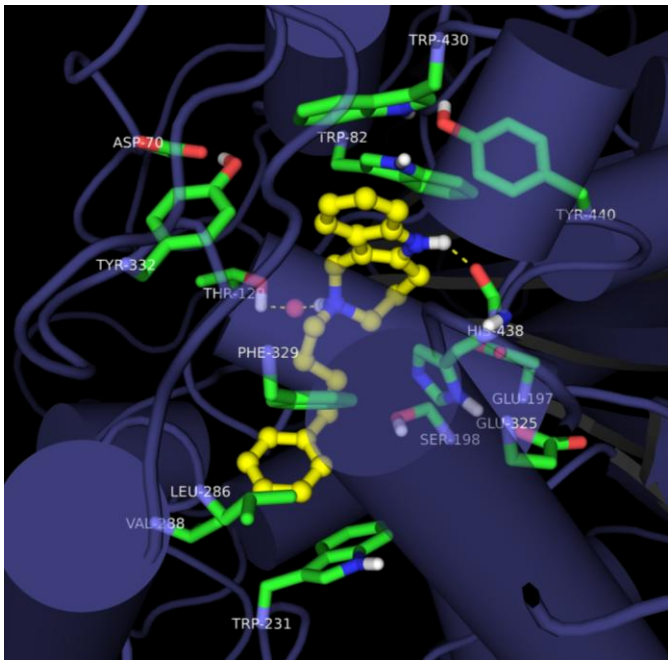

Figure 3. Binding mode of **15d** into the human BChE binding site (the free energy of binding calculated with hydration force field of AutoDock is -8.08 kcal/mol, while the contact surface area measures 717.52 Å^2).

The same docking calculation protocol was applied to simulate the binding mode of **15d** to *hu*AChE. The observed selectivity was substantially justified by docking results (see Supp. Info.), which showed lower stabilizing interactions with Trp286 in *hu*AChE.

2.5 Additional anti-AD properties

2.5.1. $A\beta_{1\text{-}40}$ aggregation assay

In current approaches, small molecules able to inhibit ChEs and Aβ aggregation/neurotoxicity simultaneously may have therapeutic potential as anti-AD agents [50-52]. Herein, the most potent BChE-selective inhibitors (Table 4) were assayed for their ability to inhibit self-induced aggregation of $A\beta_{1\text{-}40}$ through a test measuring thioflavin T (ThT) fluorescence [53]. Quercetin, as strong in vitro inhibitor of Aβ aggregation, was used as positive control. All the tested compounds, significantly less active than quercetin, behaved as moderate inhibitors of Aβ aggregation, with % inhibition at 100 μM concentration between 38 and 54%, without apparent dependence upon the length N^2-phenylalkyl group (Fig. 4). Several aza-heterocyclic derivatives endowed with in vitro antiaggregating activity were reported in literature, and the anti-Aβ pharmacophore consists in a planar heterocyclic scaffold (that is the intercalating moiety for β-sheet disruption) suitably decorated with small polar and H-bonding groups (OH, OMe, etc.) [53]. Most likely, compared to quercetin and heterocyclic analogs, the lower activity of the HHAI derivatives may be mainly due to the lack of OH groups in suitable positions.

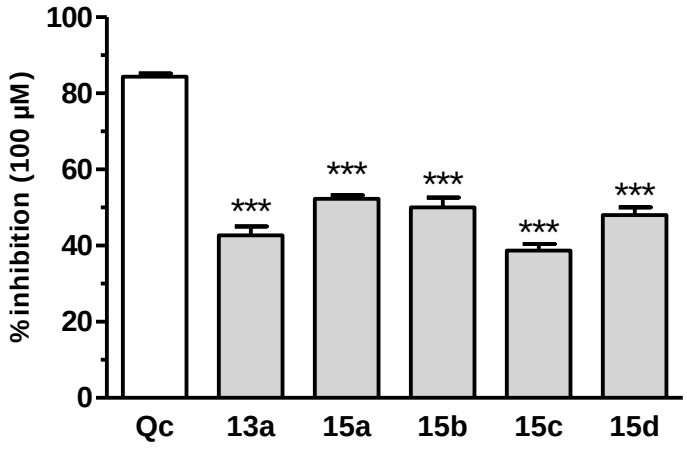

Figure 4. Percent inhibition of $A\beta_{40}$ aggregation (mean ± SD) of *N*-phenylalkyl-HHAI derivatives at 100 μM concentration; quercetin (Qc, 100 μM) used as positive control. Significant difference from positive control (ANOVA): *** $P < 0.001$

2.5.2. Neuroprotective activity against $A\beta_{1-42}$ and ROS

The in vitro neuroprotection in SH-SY5Y cell line against $A\beta_{42}$-induced cytotoxicity for **15d** was measured through an MTT assay on a cell model, without considering the molecular events triggering neurotoxicity [53, 54]. As shown in Fig 5, the aggregates formed by 5 μM Aβ in cultured SH-SY5Y cells produced around 50% of cell death in two days. According to the observed anti-Aβ aggregation activity, cells co-incubated with equimolar (5 μM) $A\beta_{42}$ and **15d** exhibited a significantly reduced decline of cell viability, after 24 h (35% viability recovery) and 48 h (30% viability recovery) as hallmark of neuroprotection. Compound **15d**, tested alone at the same concentration, showed own cytotoxicity (ca. 30% decrease in cell viability) only after 48 h, while maintaining a significant protecting effect against Aβ-induced toxicity, which resulted slightly lower than that observed at 24 h. The observed time-dependent effect may be ascribed to physical and/or chemical (metabolic) stability of **15d**.

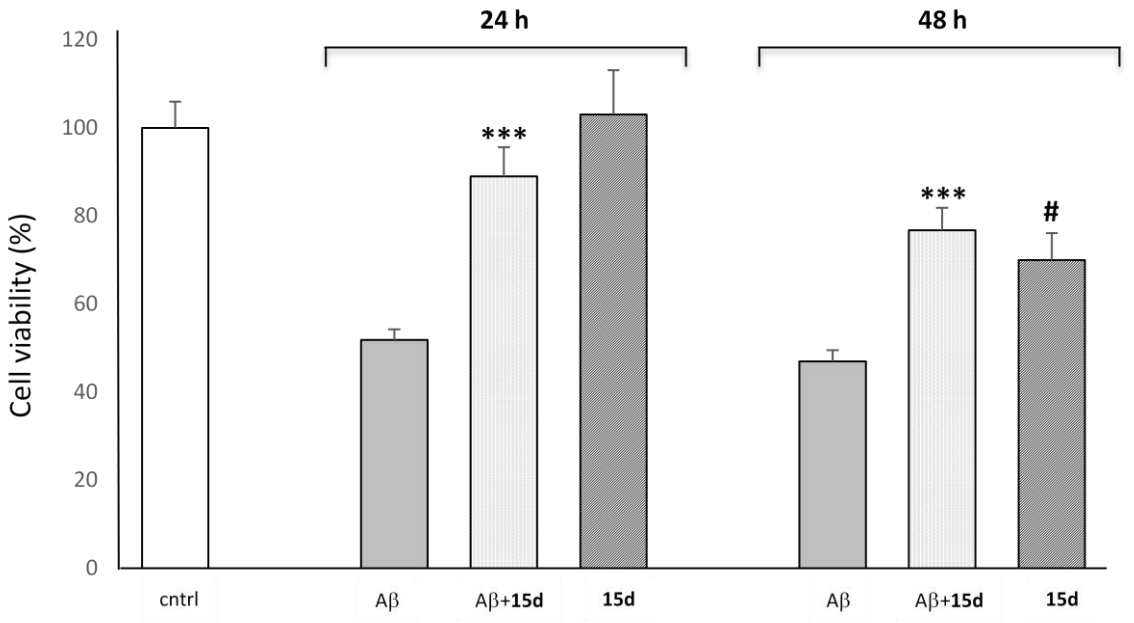

Figure 5. Cytoprotection in SH-SY5Y cells of compound **15d** (5 μM) as assessed by MTT cell viability assay, after treatment with $A\beta_{1-42}$ (5 μM). Values are expressed as mean ± S.E.M. of six replicates; significantly different from untreated cells and $A\beta_{1-42}$ (5 μM) alone, as estimated by ANOVA: $^{\#}P < 0.05$ vs untreated cells; $^{***}P < 0.001$ vs $A\beta_{1-42}$ (5 μM) alone.

Cytoprotective effect against oxidative stress cell damage was also investigated in H_2O_2-induced oxidation SH-SY5Y cell model (Fig. 6). Reactive oxygen species (ROS) production was detected by means of a spectrofluorometric measure of the fluorescent probe 2′,7′-dichlorofluorescein (DCFH) [53]. Quercetin, a well-known natural antioxidant, was used as reference compound.

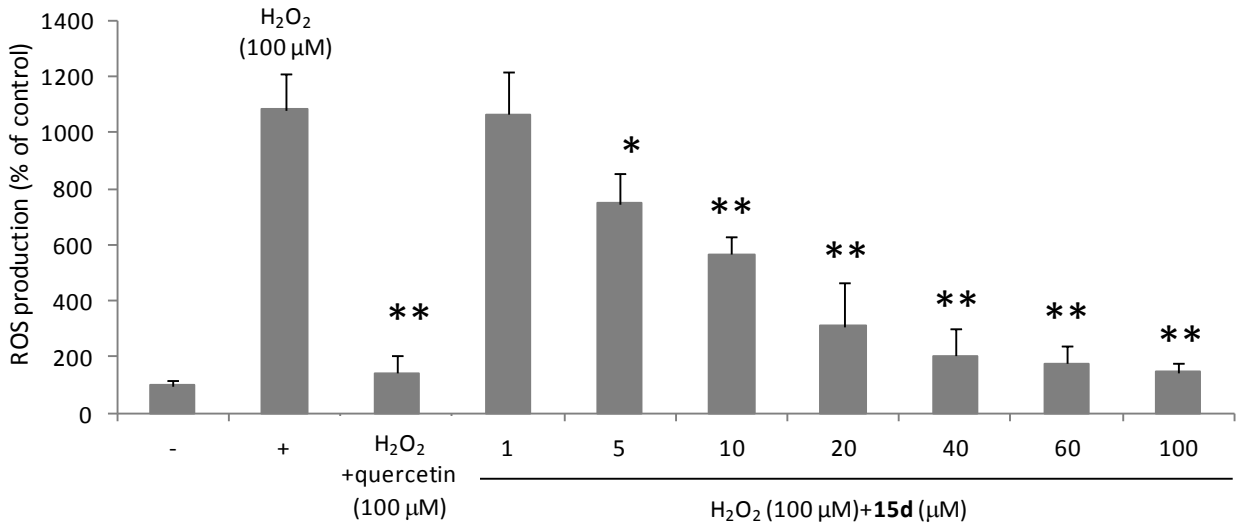

Figure 6. Radical scavenging activity of increasing concentrations of **15d** on SH-SY5Y cell line, after H_2O_2 (100 µM) induced cell damage (DCFH-DA) assay; (-) untreated cells; (+) H_2O_2-treated cells. Values are expressed as mean ± S.E.M. from six replicates; significantly different from H_2O_2-treated cells: $^{*}P < 0.01$, $^{**}P < 0.0001$.

A dose-dependent ROS-scavenging effect of **15d** was observed after coincubation of the test compound at different concentrations (1-100 µM) with 100 µM H_2O_2. Interestingly, the protection activity of **15d** from H_2O_2-induced oxidative stress was statistically significant at concentrations higher than 5 µM, and comparable to that of 100 µM quercetin at even lower concentrations (40 µM). The calculated IC_{50} was equal to 10.1 ± 1.2 µM. The data suggested an antioxidant activity of **15d**, an effect which should not be surprising, considering that tertiary amines, like **15d**, react in aqueous solvents with peroxides leading to formation of quaternary *N*-oxides [55], including some bioreductive drugs [56].

The aqueous solubility of compound **15d** (as well as **15a** and **15c**), experimentally measured [57,58], was found higher than 1 mM. The same compounds were predicted by the 'admetSAR' software [59] as potentially able to cross blood brain barrier (BBB) [60,61], non-hepatotoxic and well absorbed through human intestine [62]. Physicochemical descriptors and ADMET parameters are reported in Supporting Information.

3. Conclusions

About twenty derivatives of 1,2,3,4,5,6-hexahydroazepino[4,3-*b*]indole (HHAI) were evaluated in vitro as inhibitors of ChEs and amyloid Aβ aggregation. A structure-activity relationship study, mostly exploring substitutions at the azepine nitrogen with groups having different size and lipophilicity, led to find out N^2-phenylalkyl HHAI derivatives (**15**) which achieved inhibition of *hs*BChE at submicromolar concentrations and ten-to-hundred selectivity over *ee*AChE. The most potent N^2-phenylbutyl compound **15d** behaved as a mixed-type inhibitor and showed in vitro inhibitory activity (IC_{50} ca. 0.2 μM) and selectivity (> 100-fold) also towards human BChE. Molecular docking calculation of **15d** into the binding site of BChE suggested π-stacking interactions (involving Trp82 and Trp231) and two hydrogen bonds (with Thr120 side chain and His438 carbonyl in the backbone) as important for the good inhibitory activity. Finally, **15d** exhibited significant ($P < 0.001$) protection activity on neuroblastoma SH-SY5Y cell line against cytotoxicity induced by $A\beta_{42}$ peptide and oxidative stress (hydrogen peroxide). Taking these properties into account, the HHAI moiety can be considered a useful template for developing new molecules inhibiting BChE, which is a promising drug target in advanced AD. Compound **15d**, showing additional anti-Aβ and anti-oxidative stress in neuronal cell culture, can be a candidate for advancing in molecular optimization and in vivo pharmacological studies aimed at assessing its potential as MTDL in the management of multifactorial AD-related neurodegeneration.

4. Experimental methods

Starting materials and all chemicals and solvents were purchased from Sigma-Aldrich and Alfa Aesar. Melting points were determined by using the capillary method on a Stuart Scientific SMP3 electrothermal apparatus and are uncorrected. Final compound purities were assessed by elemental analyses (C, H, N), performed on Euro EA3000 analyzer (Eurovector, Milan, Italy) by the Analytical Laboratory Service of the Department of Pharmacy-Drug Sciences of the University of Bari (Italy), and the results agreed to within ±0.40% of theoretical values. Mass spectra were obtained by Agilent 1100 Series LC-MSD Trap System VL, equipped with ESI (electrospray ionization) source (Agilent Technologies Italia S.p.A., Cernusco sul Naviglio, Milan, Italy). The high-resolution molecular masses of test compounds were assessed by Agilent 6530 Accurate Mass Q-TOF (Agilent Technologies Italia S.p.A., Cernusco sul Naviglio, Milan, Italy). IR spectra (KBr disks) were recorded on a Perkin-Elmer Spectrum One Fourier transform infrared spectrophotometer (Perkin-Elmer Ltd., Buckinghamshire, U.K.), and the most significant absorption bands are listed. ^{1}H NMR spectra, Unless otherwise stated, were recorded at 300 MHz on a Varian Mercury 300 instrument. Chemical shifts are expressed in δ and the coupling constants *J* are in hertz (Hz); the following abbreviations are used: s, singlet; d, doublet; dd, doublet-doublet; t, triplet; m, multiplet. Signals due to NH and OH protons were located by deuterium exchange with D_2O. Chromatographic separations were performed on silica gel 60 for column chromatography (Merck 70-230 mesh, or alternatively 15-40 mesh for flash chromatography).

Tetrahydro- (**7a-c)**, and hexahydroazepinoindoles (**8a-c**), and compounds **10a-b**, **11a-d, 13a-c**, and **16** were synthesized according to procedures reported by us or described elsewhere [35,45,46,47,48]. Analytical and spectral data of newly synthesized and tested compounds (**13d-h**, and **15a-d**), and their intermediates, are described below, and in Supporting Information.

*4.1 General procedure A: preparation of 1,2,3,4,5,6-hexahydroazepino[4,3-b]indoles (**8a-c**)*

*4.1.1 Synthesis of 1,2,3,4,5,6-hexahydroazepino[4,3-b]indole (**8a**),*

The preparation of 1,2,3,4,5,6-hexahydroazepino[4,3-b]indole (**8a**), previously synthesized,[46,47] has been reported as a representative example. To a stirred solution of 3,4,5,6-tetrahydroazepino[4,3-*b*]indol-1(2*H*)-one **7a**[45] (300 mg, 1.5 mmol), preheated and refluxed in 60 mL of dry 1,4-dioxane up to complete solubilization, was added portionwise lithium aluminium hydride (625 mg, 16.5 mmol), and mixture was refluxed under nitrogen atmosphere, until disappearance of starting material was observed (TLC, about 20 hours). After cooling, mixture was quenched by adding 20 mL of Na_2SO_4 saturated aqueous solution, and stirred 30 minutes at room temperature. Residue was filtered off and washed with 1,4-dioxane. The filtrates were diluted with 100 mL of water, and the organic/aqueous mixture was extracted with chloroform (3 × 50 mL). Collected organic phases were washed twice with 20 mL of brine, dried (anhydrous Na_2SO_4), filtered and concentrated under reduced pressure, to obtain compound **8a**, as a brown solid, which was further used without purification. Spectral data were in agreement with those of literature. Yield: 90% (GC). IR (KBr) ν: 3416, 3276, 1621, 1448 cm^{-1}; ^1H NMR (300 MHz, DMSO-d_6) δ: 10.74 (br, 1H), 7.36 (d, *J* = 8.0 Hz, 1H), 7.24 (d, *J* = 8.0 Hz, 1H), 6.97 (t, *J* = 8.0 Hz, 1H), 6.92 (t, *J* = 8.0 Hz, 1H), 3.88 (s, 2H), 3.06 (dd, *J1* = 6 Hz, *J2* = 7.5 Hz, 2H), 3.03 (br, 1H), 2.90 (dd, *J1* = 6Hz, *J2* = 7 Hz, 2H), 1.76 (m, 2H).

9-fluoro-1,2,3,4,5,6-hexahydroazepino[4,3-*b*]indole (**8b**) and 9-methyl-1,2,3,4,5,6-hexahydroazepino[4,3-*b*]indole (**8c**) were prepared by following the same synthetic conditions; spectral data were in agreement with those of literature.[36,46]

4.2 General procedure B: preparation of 2-(phenacyl)-1,2,3,4,5,6-hexahydroazepino[4,3-b]indole (**9**-**10**-**11**)

*4.2.1. Synthesis of 2-(*1-phenyl-2-(3,4,5,6-tetrahydroazepino[4,3-*b*]indol-2(1H)-yl)ethanone (**9e**)

The preparation of *2-(*1-phenyl-2-(3,4,5,6-tetrahydroazepino[4,3-*b*]indol-2(1H)-yl)ethanone (**9e**), has been reported as a representative example.

To a solution of phenylacetic acid (570 mg, 4.17 mmol), in 10 mL of fresh distilled dry THF was added thionyl chloride ($SOCl_2$, 0.30 mL, 4.30 mmol). The mixture was refluxed 3 hours, and after cooling dried under N_2 stream. The crude residue was dissolved in 10 mL of fresh distilled dry methylene chloride (DCM) and added dropwise to an ice bath cooled solution of compound **8a** (518 mg, 2.78 mmol), and TEA (0.80 mL, 5.73 mmol). Mixture was stirred overnight at room temperature, and then diluted with 20 mL of DCM. The organic phase was washed with saturated aqueous Na_2CO_3 (3×15 mL), 1N diluted HCl (3×15 mL), and brine (3×15 mL), then dried (anhydrous Na_2SO_4), filtered and concentrated under reduced pressure. The residue oil was purified by chromatography on silica gel (ethyl acetate/n-hexane 70/30 v/v) to afford compound **9e**. Yield: 37% (315 mg), pale brown oil; IR (KBr) ν: 3278, 2923, 1614, 1232, 851, 742 cm^{-1}; ^{1}H-NMR (300 MHz, $CDCl_3$) δ: 7.93 (s, 1H), 7.46 (dd, *J1* = 3.3 Hz, *J2* = 6 Hz, 1H), 7.38 - 7.21 (m, 6H), 7.17 - 7.12 (m, 2H), 4.62 (s, 2H), 3.90 (t, *J* = 5.8 Hz, 2H), 3.70 (s, 2H), 2.94 (t, *J* = 6.0 Hz, 2H), 2.10 - 2.00 (m, 2H).

*4.3 Synthesis of 6-methyl-2-(3-phenylpropanoyl)-1,2,3,4,5,6-hexahydroazepino[4,3-b]indole (**14a**)*

TBAB (276 mg, 0.85 mmol), methyl iodide (0.20 mL, 2.85 mmol) and 5.0 mL of 50% m/v NaOH were added to a solution of **9e** (175 mg, 0.57 mmol) in 5 mL of dry DCM. The mixture was stirred overnight at room temperature, and then diluted with 20 mL of DCM and 20 mL of water. The collected organic phase was washed twice with 20 mL of brine, dried (Na_2SO_4), filtered and concentrated under reduced pressure. The residue was purified by chromatography on silica gel (ethyl acetate/*n*-hexane 80/20 v/v, as eluent), to afford compound **14a**. Yield: 79% (150 mg), pale yellow oil; IR (KBr) ν: 3029, 2938, 1635, 1471, 910, 734 cm^{-1}; ^{1}H-NMR (300 MHz, $CDCl_3$) δ: 7.48 (d, *J* = 6.8 Hz, 1H), 7.35 - 7.5 (m, 8H), 4.62 (s, 2H), 3.94 (t, *J* = 5.8 Hz, 2H), 3.67 (s, 3H), 2.98-2.85 (m, 2H), 2.16-2.10 (m, 2H).

4.4 General procedure C: preparation of 2-(phenylalkyl)-1,2,3,4,5,6-hexahydroazepino[4,3-b]indole as hydrochloride salts (**13a-g**, **15a-d**)

*4.4.1. Synthesis of 2-(2-phenylethyl)-1,2,3,4,5,6-hexahydroazepino[4,3-b]indole hydrochloride (**15a**).*

The preparation of compound **15a**, has been reported as a representative example. To a 0 °C ice bath cooled solution of compound **9e** (330 mg, 1.09 mmol) in 50 mL of fresh distilled dry THF anidro, $LiAlH_4$ (227 mg, 5.97 mmol) was added portionwise, and the mixture was refluxed overnight, until starting material disappearance. After cooling, mixture was quenched by adding 10 mL of Na_2SO_4 saturated aqueous solution and stirred 30 minutes at room temperature. Residue was filtered off and washed with 1,4-dioxane. The filtrates were collected and dried under reduced pressure. The obtained oil residue was suspended in 50 mL of distilled water, and aqueous mixture was extracted with chloroform (3 × 50 mL). Collected organic phases were washed twice with 20 mL of brine, dried (anhydrous Na_2SO_4), filtered and concentrated under reduced pressure. The residue oil was purified by chromatography on silica gel (ethyl acetate/MeOH 70/30 v/v) to afford a brown oil, which was stirred 2 hours in HCl saturated methanol solution. After solvent removal, and crystallization of solid residue (EtOH/Ethyl acetate) compound **15a**, as hydrochloride salt. Yield: 56% (200 mg); brown solid, mp 125-127 °C; IR (KBr): ν = 3399, 3261, 2695, 2616, 1629, 1456, 747 cm^{-1}; ^{1}H-NMR (300 MHz, d_6-DMSO) δ: 11.46 (s, 1H), 10.77 (s, 1H), 7.63 (dd, *J1* = 6.0 Hz, *J2* = 2.0 Hz, 1H), 7.40 - 6.90 (m, 8H), 4.69 (d, *J* = 14.5 Hz, 1H), 4.59 (dd, *J1* = 14.5 Hz, *J2* = 5.0 Hz, 1H), 3.68 (dd, *J1* = 12.0 Hz, *J2* = 9.0 Hz, 1H), 3.62-3.35 (m, 3H), 3.20 - 2.80 (m, 4H), 2.20 - 1.90 (m, 2H); ^{13}C-NMR (300 MHz, d_6-DMSO) δ: 140.77,137.54, 129.16, 128.42, 127.15, 121.15, 119.88, 117.54, 111.34, 101.17, 79.69, 57.14, 55.30, 53.85, 48.76, 30.24, 26.37, 22.19; HRMS calcd for $C_{20}H_{23}N_2$ $[M+H]^+$ 291.1856, found 291.1844. Anal $C_{20}H_{22}N_2 \times HCl$ (C, H, N).

*4.4.2. Synthesis of 2-(benzyl)-1,2,3,4,5,6-hexahydroazepino[4,3-b]indole hydrochloride (**13a**)*

Compound **13a** was obtained as described for compound **15a**, by following the general procedure C. The residue oil was purified by chromatography on silica gel (ethyl acetate/MeOH 70/30 v/v). Obtained hydrochloride salt of **13a**. Yield: 76% (80 mg); brown solid, mp 105-107 °C; IR (KBr) ν: 3432, 1624, 1440, 1380, 800, 740 cm^{-1}; ^{1}H-NMR (300 MHz, d_6-DMSO) δ: 11.38 (s, 1H), 9.60 (s, 1H), 7.60-7.40 (m, 3H), 7.18-7.10 (m, 2H), 7.24 (d, *J* = 8.0 Hz, 2H), 7.06 - 6.99 (m, 2H), 4.29 (dt, *J1* = 4.0 Hz, *J2* =15 Hz, 2H), 3.70 (d, *J* = 15.0 Hz, 2H), 3.05-2.90 (m, 2H), 2.20 - 2.10 (m, 2H), 2.10-2.00 (m, 2H); ^{13}C-NMR (300 MHz, d_6-DMSO) δ: 140.06, 138.72, 134.60, 129.10 (2C), 128.75, 128.49 (2C), 127.16, 120.01, 118.58, 117.06, 111.05, 109.88, 59.03, 58.36, 49.92, 28.00, 25.14; HRMS calcd for $C_{19}H_{21}N_2$ $[M+H]^+$ 277.1699, found 277.1702. Anal $C_{19}H_{20}N_2 \times HCl$ (C, H, N).

4.4.3. Synthesis of 2-(4-methylbenzyl)-1,2,3,4,5,6-hexahydroazepino[4,3-b]indole hydrochloride ***(13d)***

Compound **13d** was obtained as described for compound **15a**, by following the general procedure C. The residue oil was purified by chromatography on silica gel (ethyl acetate/MeOH 70/30 v/v). Obtained hydrochloride salt of **13d**. Yield: 78% (84 mg); brown solid, mp 105-106 °C; IR (KBr) ν: 3433, 1626, 1442, 1384, 876, 742 cm^{-1}; ^{1}H-NMR (300 MHz, d_6-DMSO) δ: 11.40 (s, 1H), 10.30 (s, 1H), 7.43 (d, *J* = 8.0 Hz, 2H), 7.32 (d, *J* = 7.0 Hz, 2H), 7.24 (d, *J* = 8.0 Hz, 2H), 7.06 - 6.99 (m, 2H), 4.64 (d, *J* = 15.0 Hz, 1H), 4.29 (dt, *J1* = 4.0 Hz, *J2* =15 Hz, 2H), 4.20 (d, *J* = 15.0 Hz, 1H), 3.70 - 3.45 (m, 2H), 2.99 (t, *J* = 5.5 Hz, 2H), 2.33 (s, 3H), 2.20 - 2.10 (m, 1H), 2.10-2.00 (m, 1H); ^{13}C-NMR (300 MHz, d_6-DMSO) δ: 140.76, 139.30, 134.83, 131.65, 129.71, 128.24, 127.67, 121.10, 119.54, 117.32, 111.60, 101.03, 56.66, 56.40, 48.61, 26.19, 22.45, 21.29; HRMS calcd for $C_{20}H_{23}N_2$ $[M+H]^+$ 291.1856, found 291.1854. Anal $C_{20}H_{22}N_2 \times HCl$ (C, H, N).

4.4.4. Synthesis of 2-(4-fluorobenzyl)-1,2,3,4,5,6-hexahydroazepino[4,3-b]indole hydrochloride ***(13e)***

Compound **13e** was obtained as described for compound **15a**, by following the general procedure C. The residue oil was purified by chromatography on silica gel (ethyl acetate/MeOH 70/30 v/v). Obtained hydrochloride salt of **13e**. Yield: 40% (160 mg); brown solid, mp 100-102 °C; IR (KBr) ν: 3430, 2937, 2586, 1605, 1432, 1228, 876, 744 cm^{-1}; ^{1}H-NMR (300 MHz, d_6-DMSO) δ: 11.42 (s, 1H), 10.33 (s, 1H), 7.65 - 7.60 (m,2H), 7.37 - 7.20 (m, 2H), 7.02 (quintet, *J* = 8.0 Hz, 2H), 4.62 (d, *J* = 14.0 Hz, 1H), 4.35 - 4.20 (m, 3H), 3.59 (dd, *J1* = 12.0 Hz, *J2* = 9.0 Hz, 1H), 3.38 (dd, *J1* = 12.0 Hz, *J2* = 9.0 Hz, 1H), 3.05 - 2.95 (m, 2H), 2.25-2.10 (m, 1H), 2.10-1.90 (m, 1H)); ^{13}C-NMR (300 MHz, d_6-DMSO) δ: 164.00, 162.04, 140.91, 134.79, 134.16, 128.21, 127.07, 121.11, 119.57, 117.30, 116.14, 115.97, 111.61, 100.85, 56.46, 55.73, 48.47, 26.43, 22.31; HRMS calcd for $C_{19}H_{20}N_2F$ $[M+H]^+$ 195.1605, found 295.1611. Anal $C_{19}H_{19}N_2F \times HCl$ (C, H, N).

*4.4.5. Synthesis of 9-fluoro-2-(4-fluorobenzyl)-1,2,3,4,5,6-hexahydroazepino[4,3-b]indole hydrochloride (**13f**)*

Compound **13f** was obtained as described for compound **15a**, by following the general procedure C. The residue oil was purified by chromatography on silica gel (ethyl acetate/MeOH 70/30 v/v). Obtained hydrochloride salt of **13f**. Yield: 40% (155 mg); brown solid, mp 96-99 °C; IR (KBr) ν:3271, 2956, 2750, 1237, 830, 701 cm^{-1}H-NMR (300 MHz, d_6-DMSO) δ: 11.35 (s, 1H), 10.29 (s, 1H), 7.32 (dd, *J1* = 4.0 Hz, *J2* = 9.0 Hz, 1H), 7.22 (d, *J* = 8.5 Hz, 2H), 7.12 (d, *J* = 9.0 Hz, 1H), 7.05 (t, *J* = 8.0 Hz, 2H), 6.88 (t, *J* = 9.0 Hz, 1H), 4.60 (s, 2H), 4.05 (t, *J* = 5.0 Hz, 2H), 3.06 (t, *J* = 5.5 Hz, 2H), 2.20 - 2.10 (m, 2H); ^{13}C-NMR (300 MHz, d_6-DMSO) δ: 160.79, 158.28, 141.25, 135.99, 131.31, 130.81 (2C),128.96, 115.28 (2C), 111.87, 110.34, 107.90, 102.03, 57.91, 57.71, 49.75, 28.06, 24.73; HRMS calcd for $C_{19}H_{19}N_2F_2$ $[M+H]^+$ 33.1511, found 313.1521. Anal $C_{19}H_{18}N_2F_2 \times HCl$ (C, H, N).

*4.4.6. Synthesis of N,N-diethyl-N-{4-[(9-fluoro-1,2,3,4,5,6-hexahydroazepino[4,3-b]indol-2(1H)-yl)methyl]benzyl}amine dihydrochloride (**13g**)*

Compound **13g** was obtained as described for compound **15a**, by following the general procedure C. The residue oil was purified by chromatography on silica gel (DCM/MeOH 90/10 v/v). Obtained dihydrochloride salt of **13g**. Yield: 50% (180 mg); black oil; IR (KBr) ν: 3331, 3275, 2750, 1200, 810, 700 cm^{-1}. ^{1}H-NMR (300 MHz, d_6-DMSO) δ: 11.70 (s, 1H), 10.50 (s br, 1H), 10.38 (s br, 1H), 7.80-7.55 (m, 4H), 7.30 (dd, *J1* = 4.5 Hz, *J2* = 9.0 Hz, 1H), 7.05 (d, *J* = 9.0 Hz, 1H), 6.87 (t, *J* = 9.0 Hz, 1H), 4.52 (d, *J* = 15.0 Hz, 1H), 4.45-4.05 (m, 9H), 3.15-2.90 (m, 4H), 2.20-2.00 (m, 2H), 1.24 (t, *J* = 7.0 Hz, 6H)); ^{13}C-NMR (300 MHz, d_6-DMSO) δ: 158.47, 156.63, 143.15, 133.14, 131.93 (2C), 131.62, 131.47, 131.19 (2C), 128.76, 112.55, 109.80, 102.55, 56.44, 56.32, 55.71, 52.99, 52.82, 48.55, 26.43, 23.02 (2C), 22.05; HRMS calcd for $C_{24}H_{31}N_3F$ $[M+H]^+$ 380.2497, found 380.2499.

*4.4.7. Synthesis of 2-[4-(pyrrolidin-1-ylmethyl)benzyl]-1,2,3,4,5,6-hexahydroazepino[4,3-b]indole dihydrochloride (**13h**)*

Compound **13h** was obtained as described for compound **15a**, by following the general procedure C. The residue oil was purified by chromatography on silica gel (DCM/MeOH 90/10 v/v). Obtained dihydrochloride salt of **13h**. Yield: 37% (135 mg); pale brown oil; IR (KBr) ν: 3290, 3277, 2755, 1205, 807, 705 cm^{-1}; ^{1}H-NMR (300 MHz, d_6-DMSO) δ: 11.49 (s, 1H), 10.49 (s br, 1H), 10.22 (s br, 1H), 7.73-7.55 (m, 4H), 7.32 (dd, *J1* = 4.5 Hz, *J2* = 9.0 Hz, 1H), 7.09 (dd, *J1* = 3.0 Hz, *J2* = 9.0 Hz, 1H), 6.89 (t, *J1* = 9.0 Hz, 1H), 4.65 (d, *J1* = 14.0 Hz, 1H), 4.45-4.25 (m, 9H), 3.55-3.45 (m, 2H), 3.10-2.90 (m, 2H), 2.09-1.78 (m, 6H); ^{13}C-NMR (300 MHz, d_6-DMSO) δ: 158.49, 156.81, 143.12, 133.11, 132.00 (2C), 131.60, 131.47, 131.15 (2C), 128.81, 112.63, 109.77, 102.59, 57.42, 57.30, 52.11, 48.70, 45.71, 42.87, 28.77, 26.43, 18.32, 18.09; HRMS calcd for $C_{24}H_{29}N_3F$ $[M+H]^+$ 378.2340, found 378.2341.

*4.4.8. Synthesis of 6-methyl-2-(2-phenylethyl)-1,2,3,4,5,6-hexahydroazepino[4,3-b]indole hydrochloride (**15b**)*

Compound **15b** was obtained as described for compound **15a**, by following the general procedure C. The residue oil was purified by chromatography on silica gel (ethyl acetate/MeOH 75/25 v/v). Obtained hydrochloride salt of **15b**. Yield: 66% (70 mg); brown solid, mp 98-100 °C; IR (KBr) ν: 3399, 2695, 2616, 1629, 1456, 747 cm^{-1}; ^{1}H-NMR (300 MHz, d_6-DMSO) δ: 10.75 (s, 1H), 7.65 (dd, *J1* = 6.0 Hz, *J2* = 2.0 Hz, 1H), 7.40 - 6.90 (m, 8H), 4.70 (d, *J* = 14.5 Hz, 1H), 4.61 (dd, *J1* = 14.5 Hz, *J2* = 5.0 Hz, 1H), 3.70 (s, 3H), 3.65 (dd, *J1* = 12.0 Hz, *J2* = 9.0 Hz, 1H), 3.62-3.35 (m, 3H), 3.20-2.80 (m, 4H), 2.20-1.85 (m, 2H); ^{13}C-NMR (300 MHz, d_6-DMSO) δ: 140.70,137.52, 129.15, 128.45, 127.25, 121.11, 119.90, 117.52, 111.34, 101.19, 79.69, 57.12, 55.32, 53.83, 48.82, 30.29, 29.03, 26.35, 22.18; HRMS calcd for $C_{21}H_{25}N_2$ $[M+H]^+$305.2012, found 305.2013. Anal $C_{21}H_{24}N_2$ × HCl (C, H, N).

4.4.9. Synthesis of 2-(3-phenylpropyl)-1,2,3,4,5,6-hexahydroazepino[4,3-b]indole hydrochloride ***(15c)***

Compound **15c** was synthesized as described for compound **15a**, by following the general procedure C. The residue oil was purified by chromatography on silica gel (ethyl acetate/MeOH 90/10 v/v), and converted into the corresponding hydrochloride salt of **15c**. Yield 56% (202 mg), brown solid; m.p. 143-144 °C; IR (KBr): ν; 3330, 1628, 738, 713, 700 cm^{-1}; ^{1}H-NMR (300 MHz, d_6-DMSO) δ: 11.38 (s, 1H), 10.28 (s, 1H), 7.51 (d, J= 7 Hz, 1H), 7.35-7.20 (m, 3H), 7.22-7.10 (m, 3H), 7.08-6.88 (m, 2H), 4.60-4.40 (m, 2H), 3.70-3.55 (m, 1H), 3.50-3.35 (m, 1H), 3-05-2.85 (m, 4H), 2.53 (t, J=7Hz, 2H), 2.10-1.90 (m, 2H), 1.62-1.43 (m, 2H); ^{13}C-NMR (300 MHz, d_6-DMSO) δ: 140.70, 136.43, 134.80, 128.82 (2C), 128.62 (2C), 126.51, 122.83, 121.14, 119.66, 117.45, 111.97, 111.58, 57.13, 52.78, 48.65, 38.26, 32.47, 26.37, 23.90; HRMS calcd for $C_{21}H_{25}N_2$ $[M+H]^+$305.2012, found 305.2011. Anal $C_{21}H_{24}N_2$ × HCl (C, H, N).

4.4.10. Synthesis of 2-(4-phenylbutyl)-1,2,3,4,5,6-hexahydroazepino[4,3-b]indole hydrochloride ***(15d)***

Compound **15d** was synthesized as described for compound **15a**, by following the general procedure C. The residue oil was purified by chromatography on silica gel (ethyl acetate/MeOH 90/10 v/v), and converted into the corresponding hydrochloride salt of **15d**. Yield 66% (315 mg), dark brown solid; m.p. 165-167 °C; IR (KBr) ν: 3430, 3152, 2952, 2579, 1621, 1523, 1452, 1384, 1354 cm^{-1}; ^{1}H-NMR (300 MHz, d_6-DMSO) δ: 11.40 (s, 1H), 10.27 (s, 1H), 7.50 (d, J= 7 Hz, 1H), 7.32-7.21 (m, 3H), 7.20-7.10 (m, 3H), 7.10-6.90 (m, 2H), 4.60-4.40 (m, 2H), 3.70-3.55 (m, 1H), 3.50-3.35 (m, 1H), 3-05-2.85 (m, 4H), 2.53 (t, J=7Hz, 2H), 2.10-1.90 (m, 2H), 1.71 (quint., J=7.5 Hz, 2H), 1.62-1.43 (m, 2H); ^{13}C-NMR (300 MHz, d_6-DMSO) δ: 141.99, 140.67, 134.80, 128.69, 128.39, 126.26, 121.11, 119.64, 117.33, 111.53, 101.14, 57.08, 52.60, 48.38, 35.03, 28.36, 26.41, 23.75, 22.08; HRMS calcd for $C_{22}H_{27}N_2$ $[M+H]^+$ 319.2169, found 319.2167x. Anal $C_{22}H_{26}N_2 \times HCl$ (C, H, N).

4.5. Molecular modeling

The molecular skeletons of compounds **13a** and **15d**, with standard values of bond lengths and valence angles, were built using the Maestro software package (Schrödinger Release 2018-4, Maestro, Schrödinger, LLC, New York, NY, 2018), and for the most active inhibitor a conformational sampling, ensuring an energetically stable puckering of the hexahydroazepino ring, was after performed by means of OMEGA (rel. 3.0.0.1, OpenEye Scientific Software, Santa Fe, NM), generating a total of 2217 conformers, hereafter docked into the BChE binding site.

According to the high homology (*ca*. 90%) between the horse serum and human sequence, the recently published X-ray data of BChE in complex with a *N*-propargyl piperidine nanomolar inhibitor (pdb code 6F7Q) [63] was used as biomolecular target.

Chain A of the enzyme structure was passed to the Protein Preparation Wizard interface of MAESTRO for removing water molecules, and hydrogen atoms added, optimizing their position, and determining the protonation states of residues according to PROPKA prediction at pH 7.0. AMBER UNITED force field electrostatic charges [64] were applied to protein structure, whereas

for the ligand Marsili-Gasteiger charges were calculated with the molcharge suite of QUACPAC (rel. 1.7.0.2, OpenEye Scientific Software, Santa Fe, NM). For each conformer ten runs of Lamarckian Genetic Algorithm (LGA) implemented in AUTODOCK 4.2.6 [65] were performed in rigid-body docking of **15d** into the BChE binding site. To accomplish this task, affinity maps were first calculated on a 85×85×85 $Å^3$ box, 0.375 Å spaced, centered on the co-crystallized ligand, and LGA runs were issued with the tran0 (initial coordinates for the center of the ligand), quat0 (the ligand rigid-body orientation), and dihe0 (relative dihedral angles) figures set to random values. The population size and the number of energy evaluations to 150 and 5000000 respectively, taking into account water contribution according to the hydration force field of AUTODOCK [66]. Among all the plausible binding pose solutions the best one, according to the AUTODOCK free energy scoring function, was finally selected as representative of the HHAIs binding mode. For the FEP analysis the standard default protocol as implemented in the 2018-4 release of Desmond suite software package was applied to complete this task [67].

4.6. Cholinesterase inhibition assay

The test compounds were assayed for their inhibitory activity toward AChE and BChE from electric eel and horse serum, respectively, and human cholinesterases as well (Sigma-Aldrich), following the Ellman's method [49]. The BChE activity was determined in a reaction mixture containing 100 µL of a solution of BChE (0.9 U/mL in 0.1 M pH 8.0 phosphate buffer, PB), 100 µL of a solution of 5,5-dithio-bis-(2-nitrobenzoic) acid (DTNB 3.3 mM in 0.1 M pH 7.0 PB, containing 0.1 mM $NaHCO_3$), 100 µL of a solution of the test compound (five to seven concentrations, ranging from $1×10^{-4}$ to $1×10^{-9}$ M in 0.1 M pH 8.0 PB), and 600 µL of pH 8.0 PB. After incubation for 20 min at 25 °C, butyrylthiocholine iodide (100 µL of 0.05 mM water solution) was added as the substrate, and the hydrolysis rates of the substrate monitored at 412 nm for 5.0 min at 25 °C. The concentration of compound which produced 50% inhibition of the BChE activity (IC_{50}) was calculated by nonlinear regression of the response/concentration (log) curve, by using Prisma

GraphPad software (vers. 5.01). AChE inhibitory activity was determined similarly, by using a solution of AChE (0.415 U/mL in 0.1 M pH 8.0 PB), and acetylthiocholine iodide (0.05 mM) as the substrate. The inhibition data are reported as means of IC_{50}'s determined at least in three independent measurements. To determine the type of inhibition for the most potent BChE inhibitor **15d**, the Lineweaver-Burk eq (1/v vs 1/[S]) was fitted for varying concentrations of substrates (25−300 μM) in the absence or presence of inhibitor at four different concentrations, ranging from 0.5 to 0.1 μM, and by using fixed amounts of enzymes (0.18 $U \times mL^{-1}$). Replotting the slopes of the above plots against the inhibitor **15d** concentration (0.5 μM, r^2 = 0.990; 0.25 μM, r^2 = 0.977; 0.1 μM, r^2 = 0.978; no inhibitor, r^2 = 0.978) yielded the K_i value as the X-axis intercept.

4.7. Inhibition of $A\beta_{1-40}$ aggregation

The spectrofluorimetric assays, measuring ThT fluorescence in the presence of Aβ, were done as previously described [53]. Briefly, samples of Aβ were co-incubated with test molecules in PBS at 100 μM concentration containing 2% v/v of 1,1,1,3,3,3-hexafluoro-2-propanol and the antiaggregating activities were measured after 2 h of incubation at 25 °C in 96-well black, non-binding microplates (Greiner Bio-One GmbH, Frickenhausen, Germany). Fluorimetric reads were performed in a multiplate reader Infinite M1000 Pro (Tecan, Cernusco sul Naviglio, Italy). Each concentration point was run in triplicate.

4.8. Cell viability and neuroprotection assay

Cytoprotection from $A\beta_{42}$-induced neurotoxicity was assessed in SH-SY5Y cells as already described [53]. At least three independent experiments with six replicates were carried out, and the results were averaged. SH-SY5Y cells were cultured in DMEM-Dulbecco's modified Eagle's medium (Sigma-Aldrich), supplemented with 10% (v/v) inactivated fetal bovine serum, 2 mM/L, 100 μg/mL penicillin and 100 μg/mL streptomycin, at 37°C in 5% CO_2 atmosphere. For cell assays,

after grown to 70% confluence, cells were trypsinized using Trypsin-EDTA 1X in PBS (Aurogene) and plated in 96-well plates at a density of 10 000 cells per well in 125 μL of cell culture medium. To test compound **15d** for the ability to inhibit $A\beta_{1-42}$-induced toxicity, compound **15d** stock solution were prepared, and diluted with $A\beta_{1-42}$ solution in DMEM and the mixture were added quickly to cells to final concentration of 5 μM for both compound **15d** and $A\beta_{1-42}$. SH-SY5Y cell viability was determined using a conventional MTT reduction assay, based on the ability of viable cells to metabolize 3-(4,5-dimethylthiazol-2-yl)-2,5-diphenyltetrazolium bromide (MTT) (Sigma-Aldrich, Milan, Italy), a water-soluble salt (yellow color), by cellular oxidoreductase into a water-insoluble blue formazan product. Viable cells were incubated with the mixture, and at the end of incubation time (24h, 48 h), the culture medium was replaced by DMEM supplemented with a solution of MTT in PBS (50 mg/ml final concentration). After 2 h of incubation at 37 °C in 5% CO_2, this solution was removed and 125 μl of DMSO was added to each well to dissolve the product formazan. Absorbance values at 570 nm were measured using a multilabel plate counter Victor3 V (PerkinElmer), with DMSO medium as the blank solution. Data are presented as the mean ± SEM. Statistical comparisons were performed by one-way ANOVA followed by multiple comparison tests (Dunnett's test) using the statistical package in the GraphPad Prism software vers. 5.01; values of $P < 0.05$ were considered statistically significant.

4.9. Measurements of reactive oxygen species

Intracellular ROS production was evaluated using an oxidation-sensitive fluorescent probe, 2′,7′-Dichlorofluorescin diacetate (DCFH-DA; Sigma). Viable SHSY5Y cells were seeded in a black 96-well cell culture plate (PerkinElmer USA) for 24 h, and then incubated in DMEM supplemented with different concentration (ranging from 0 to 100 μM) of compound **15d** for 1 h. After removal of buffer containing **15d**, and washing, DCFH-DA (50 μM final concentration) in medium without serum was added directly to each well, and the plate was incubated 30 min at 37 °C (5% CO_2). After washing using PBS, 100 μM H_2O_2/well in PBS was added and the cells were incubated for 30

min. The formation of fluorescent dichlorofluorescein (DCF) due to oxidation of DCFH in the presence of ROS, was read directly in each well at an excitation wavelength of 485 nm and an emission wavelength of 530 nm using a multilabel plate counter Victor3 V (PerkinElmer). DMSO medium was used for control cells.

Conflict of interest

We declare that we have no conflict of interest.

Appendix A. Supporting Information

Supplementary data related to this article can be found at …

Acknowledgements

Authors gratefully acknowledge the financial support from the University of Bari (Fondi di Ateneo 2012). The financial support from MIUR, Italy (Grant PRIN 2009ESXPT2_005) is gratefully acknowledged. This work was also supported by the RUDN 5-100 program and RFBR (grant # 17-53-10012 KO_a).

References

[1] https://www.alz.co.uk/research/world-report-2018

[2] A. Kumar, A. Singh, A. Ekavali, A review on Alzheimer's disease pathophysiology and its management: an update, Pharmacol. Rep. 67 (2015) 195-203.

[3] F. Chiti, C.M. Dobson, Protein misfolding, amyloid formation, and human disease: A summary of progress over the last decade. Annu. Rev. Biochem. 86 (2017) 27–68.

[4] W.J Geldenhuys, A.S. Darvesh, Pharmacotherapy of Alzheimer’s disease: Current and future trends, Expert Rev. Neurother. 15 (2015) 3-5.

[5] P. Masson, E. Carletti, F. Nachon, Structure, activities and biomedical applications of human butyrylcholinesterase, Protein Pept. Lett. 16 (2009) 1215-1224.

[6] N.H. Greig, T. Utsuki, D.K. Ingram, Y. Wang, G. Pepeu, C. Scali, Q.S. Yu, J. Mamczarz, H.W. Holloway, T. Giordano, D. Chen, K. Furukawa, K. Sambamurti, A. Brossi, D.K. Lahiri, Selective butyrylcholinesterase inhibition elevates brain acetylcholine, augments learning and lowers Alzheimer β-amyloid peptide in rodent, Proc. Natl. Acad. Sci. USA 102 (2005) 17213-17218.

[7] S. Darvesh, M.K. Cash, G.A. Reid, E. Martin, A. Mitnitski, C. Geula, Butyrylcholinesterase is associated with β-amyloid plaques in the transgenic APPSWE/PSEN1dE9 mouse model of Alzheimer disease, J. Neuropathol. Exp. Neurol. 71 (2012) 2-14.

[8] E.G. Duysen, B. Li, S. Darvesh, O. Lockridge, Sensitivity of butyrylcholinesterase knockout mice to (-)-huperzine A and donepezil suggests humans with butyrylcholinesterase deficiency may not tolerate these Alzheimer's disease drugs and indicates butyrylcholinesterase function in neurotransmission, Toxicology 233 (2007) 60-69.

[9] T. Arendt, M.K. Bruckner, M. Lange, V. Bigl, Changes in acetylcholinesterase and butyrylcholinesterase in Alzheimer's disease resemble embryonic development - a study of molecular forms, Neurochem. Int. 21 (1992) 381-396.

[10] Q. Li, H. Yang, Y. Chen, H. Sun, Recent progress in the identification of selective butyrylcholinesterase inhibitors for Alzheimer's disease, Eur. J. Med. Chem. 132 (2017) 294-309.

[11] S. Darvesh, Butyrylcholinesterase as a Diagnostic and Therapeutic Target for Alzheimer’s Disease, Curr. Alzheimer Res. 13 (2016) 1-5.

[12] M. Bajda, A. Wieckowska, M. Hebda, N. Guzior, C.A. Sottrifer, B. Malawska, Structure-based search for new inhibitors of cholinesterases, Int. J. Mol. Sci. 14 (2013) 5608-5632.

[13] Y. Nicolet, O. Lockridge, P. Masson, J.C. Fontecilla-Camps, F. Nachon, Crystal structure of human butyrylcholinesterase and of its complexes with substrate and products, J. Biol. Chem. 278 (2003) 41141-41147.

[14] S.Y. Chiou, T.T. Weng, G.Z. Lin, R.J. Lu, S.Y. Jian, G. Lin, Molecular docking of different inhibitors and activators to butyrylcholinesterase, J. Biomol. Struct. Dyn. 33 (2014) 563-572.

[15] F.H. Darras, B. Kling, J. Heilmann, M. Decker, Neuroprotective tri- and tetracyclic BChE inhibitors releasing reversible inhibitors upon carbamate transfer, ACS Med. Chem. Lett. 3 (2012) 914-919.

[16] R. Purgatorio, M. de Candia, A. De Palma, F. De Santis, L. Pisani, F. Campagna, S. Cellamare, C.D. Altomare, M. Catto, Insights into structure-activity relationships of 3-arylhydrazonoindolin-2-one derivatives for their multitarget activity on β-amyloid aggregation and neurotoxicity. Molecules 23 (2018) E1544.

[17] D. Panek, A. Więckowska, J. Jończyk, J. Godyń, M. Bajda, T. Wichur, A. Pasieka, D. Knez, A. Pišlar, J. Korabecny, O. Soukup, V. Sepsova, R. Sabaté, J. Kos, S. Gobec, B. Malawska, Design, Synthesis, and biological evaluation of 1-benzylamino-2-hydroxyalkyl derivatives as new potential disease-modifying multifunctional anti-Alzheimer's agents. ACS Chem. Neurosci. 9 (2018) 1074-1094.

[18] D. Panek, A. Więckowska, T. Wichur, M. Bajda, J. Godyń, J. Jończyk, K. Mika, J. Janockova, O. Soukup, D. Knez, J. Korabecny, S. Gobec, B. Malawska. Design, synthesis and biological evaluation of new phthalimide and saccharin derivatives with alicyclic amines targeting cholinesterases, beta-secretase and amyloid beta aggregation. Eur. J. Med. Chem. 125 (2017) 676-695.

[19] J. Takahashi, I. Hijikuro, T. Kihara, M.G. Murugesh, S. Fuse, R. Kunimoto, Y. Tsumura, A. Akaike, T. Niidome, Y. Okuno, T. Takahashi, H. Sugimoto, Design, synthesis, evaluation and QSAR analysis of N(1)-substituted norcymserine derivatives as selective butyrylcholinesterase inhibitors. Bioorg. Med. Chem. Lett. 20 (2010) 1718-1720.

[20] J. Takahashi, I. Hijikuro, T. Kihara, M.G. Murugesh, S. Fuse, Y. Tsumura, A. Akaike, T. Niidome, T. Takahashi, H. Sugimoto, Design, synthesis and evaluation of carbamate-modified (-)-

N(1)-phenethylnorphysostigmine derivatives as selective butyrylcholinesterase inhibitors. Bioorg. Med. Chem. Lett. 20 (2010) 1721-1723.

[21] M. Shinada, F. Narumi, Y. Osada, K. Matsumoto, T. Yoshida, K. Higuchi, T. Kawasaki, H. Tanaka, Synthesis of phenserine analogues and evaluation of their cholinesterase inhibitory activities. Bioorg. Med. Chem. 20 (2012) 4901-4914.

[22] Y. Furukawa-Hibi, T. Alkam, A. Nitta, A. Matsuyama, H. Mizoguchi, K. Suzuki, S. Moussaoui, Q.S. Yu, N.H. Greig, T. Nagai, K. Yamada, Butyrylcholinesterase inhibitors ameliorate cognitive dysfunction induced by amyloid-β peptide in mice, Behav Brain Res. 225 (2011) 222-229.

[23] S. Darvesh, G.A. Reid, Reduced fibrillar β-amyloid in subcortical structures in a butyrylcholinesterase-knockout Alzheimer disease mouse model, Chem Biol Interact. 259 (2016) 307-312.

[24] K. Chalupova, J. Korabecny, M. Bartolini, B. Monti, D. Lamba, R. Caliandro, A. Pesaresi, X. Brazzolotto, A.J. Gastellier, F. Nachon, J. Pejchal, M. Jarosova, V. Hepnarova, D. Jun, M. Hrabinova, R. Dolezal, J. Zdarova Karasova, M. Mzik, Z. Kristofikova, J. Misik, L. Muckova, P. Jost, O. Soukup, M. Benkova, V. Setnicka, L. Habartova, M. Chvojkova, L. Kleteckova, K. Vales, E. Mezeiova, E. Uliassi, M. Valis, E. Nepovimova, M.L. Bolognesi, K. Kuca, Novel tacrine-tryptophan hybrids: multi-target directed ligands as potential treatment for Alzheimer's disease. Eur. J. Med. Chem. 168 (2019) 491-514.

[25] G.F. Zha, C.P. Zhang, H.L. Qin, I. Jantan, M. Sher, M.W. Amjad, M.A. Hussain, Z. Hussain, S.N. Bukhari, Biological evaluation of synthetic α,β-unsaturated carbonyl based cyclohexanone derivatives as neuroprotective novel inhibitors of acetylcholinesterase, butyrylcholinesterase and amyloid-β aggregation. Bioorg. Med. Chem. 24 (2016) 2352-2359.

[26] V. Hepnarova, J. Korabecny, L. Matouskova, P. Jost, L. Muckova, M. Hrabinova, N. Vykoukalova, M. Kerhartova, T. Kucera, R. Dolezal, E. Nepovimova, K. Spilovska, E. Mezeiova,

N.L. Pham, D. Jun, F. Staud, D. Kaping, K. Kuca, O. Soukup, The concept of hybrid molecules of tacrine and benzyl quinolone carboxylic acid (BQCA) as multifunctional agents for Alzheimer's disease. Eur. J. Med. Chem. 150 (2018) 292-306.

[27] (a) J. Leng, H.L: Qin, K. Zhu, I. Jantan, M.A. M.A. Hussain, M. Sher, M.W. Amjad, M. Naeem-Ul-Hassan, W. Ahmad, S.N. Bukhari Evaluation of multifunctional synthetic tetralone derivatives for treatment of Alzheimer's disease. Chem. Biol. Drug Des. 88 (2016) 889-898; (b) M. Wang, H.L. Qin, J. Leng, Ameeduzzafar, M.W. Amjad, M.A.G. Raja, M.A. Hussain, S.N.A. Bukhari, Synthesis and biological evaluation of new tetramethylpyrazine-based chalcone derivatives as potential anti-Alzheimer agents. Chem. Biol. Drug Des. 92 (2018) 1859-1866.

[28] G. Sinko, Z. Kovarik, E. Reiner, V. Simeon-Rudolf, J. Stojan, Mechanism of stereoselective interaction between butyrylcholinesterase and ethopropazine enantiomers. Biochimie 93 (2011) 1797-1807.

[29] G.C. González-Muñoz, M.P. Arce, B. López, C. Pérez, A. Romero, L. del Barrio, M.D. Martín-de-Saavedra, J. Egea, R. León, M. Villarroya, M.G. López, A.G. García, S. Conde, M.I. Rodríguez-Franco, N-acylaminophenothiazines: neuroprotective agents displaying multifunctional activities for a potential treatment of Alzheimer's disease. Eur. J. Med. Chem. 46 (2011) 2224-35.

[30] M. Decker, Homobivalent quinazolinimines as novel nanomolar inhibitors of cholinesterases with dirigible selectivity toward butyrylcholinesterase. J. Med. Chem. 49 (2006) 5411-5413.

[31] X. Chen, I.G. Tikhonova, M. Decker, Probing the mid-gorge of cholinesterases with spacer-modified bivalent quinazolinimines leads to highly potent and selective butyrylcholinesterase inhibitors. Bioorg. Med. Chem. 19 (2011) 1222-1235.

[32] R. Otto, R. Penzis, F. Gaube, T. Winckler, D. Appenroth, C. Fleck, C. Tränkle, J. Lehmann, C. Enzensperger, Beta and gamma carboline derivatives as potential anti-Alzheimer agents: A comparison. Eur J Med Chem. 87 (2014) 63-70.

[33] R. Ghobadian, M. Mahdavi, H. Nadri, A. Moradi, N. Edraki, T. Akbarzadeh, M. Sharifzadeh, S. N.A. Bukhari, M. Amini, Novel tetrahydrocarbazole benzyl pyridine hybrids as potent and selective butryl cholinesterase inhibitors with neuroprotective and β-secretase inhibition activities. Eur. J. Med. Chem. 155 (2018) 49-60.

[34] A.V. Varlamov, T.N. Borisova, L.G. Voskressensky, Hydrogenated pyrrolopyridines. Synthesis and reactivity, Synthesis (2002) 155-168.

[35] T.N. Borisova, L.G. Voskressensky, T.A. Soklakova, L.N. Kulikova, A.V. Varlamov, Cleavage of some annulated tetrahydropyridines under the action of dimethyl acetylene dicarboxylate in protic solvents. New practical route to substituted pyrroles and indoles, Mol. Div. 6 (2003) 207-212.

[36] L.G. Voskressensky, T.N. Borisova, T.A. Soklakova, R.S. Borisov, A.V. Varlamov, First efficient one-pot synthesis of tetrahydropyrrolo[2,3-*d*]azocines and tetrahydroazocino[4,5-*b*]indoles, Lett. Org. Chem. 2 (2005) 18-20.

[37] C Altomare, L. Summo, S. Cellamare, A.V. Varlamov, L.G. Voskressensky, T.N. Borisova, A. Carotti, Pyrrolo[3,2-*c*]pyridine derivatives as inhibitors of platelet aggregation. Bioorg. Med. Chem. Lett. 10 (2000) 581-584.

[38] L.G. Voskressensky, M. de Candia, A. Carotti, T.N. Borisova, L.N. Kulikova, A.V. Varlamov, C. Altomare, Investigation on the antiplatelet activity of pyrrolo[3,2-*c*]pyridine-containing compounds. J. Pharm. Pharmacol. 55 (2003) 323-332.

[39] M. de Candia, C. Altamura, N. Denora, S. Cellamare, M. Nuzzolese, D. de Vito, L.G. Voskressensky, A.V. Varlamov, C.D. Altomare, Physicochemical properties and antimicrobial activity of new spirocyclic thieno[2,3-*d*]pyrimidin-4(3*H*)-one derivatives. Chem. Heterocycl. Compd. 53 (2017) 357-363.

[40] R. Soto-Otero, E. Méndez-Álvarez, S. Sánchez-Iglesias, F.I. Zubkov, L.G. Voskressensky, A.V. Varlamov, M. de Candia, C. Altomare, Inhibition of 6-hydroxydopamine-induced oxidative damage by 4,5-dihydro-3*H*-2-benzazepine N-oxides. Biochem. Pharmacol. 75 (2008) 1526-1537.

[41] R. Soto-Otero, E. Méndez-Álvarez, S. Sánchez-Iglesias, J.L. Labandeira-García, J. Rodríguez-Pallares, F.I. Zubkov, V.P. Zaytsev, L.G. Voskressensky, A.V. Varlamov, M. De Candia, F. Fiorella, C. Altomare, 2-Benzazepine nitrones protect dopaminergic neurons against 6-hydroxydopamine-induced oxidative toxicity. Arch. Pharm. (Weinheim) 345 (2012) 598-609.

[42] L.G. Voskressensky, T.N. Borisova, L.N. Kulikova, A.V. Varlamov, M. Catto, C. Altomare, A. Carotti, Tandem cleavage of hydrogenated β- and γ-carbolines - New practical synthesis of tetrahydroazocino[4,5-*b*]indoles and tetrahydroazocino[5,4-*b*]indoles showing acetylcholinesterase inhibitory activity. Eur. J. Org. Chem. 14 (2004) 3128-3135.

[43] A. Carotti, M. de Candia, M. Catto, T.N. Borisova, A.V. Varlamov, E. Méndez-Álvarez, R. Soto-Otero, L.G. Voskressensky, C. Altomare, Ester derivatives of annulated tetrahydroazocines: A new class of selective acetylcholinesterase inhibitors. Bioorg. Med. Chem. 14 (2006) 7205-7212.

[44] L.G. Voskressensky, S.A. Kovaleva, T.N. Borisova, A.B. Eresko, V.S. Tolkunov, A.V. Listratova, M. de Candia, C. Altomare, A.V. Varlamov, Recyclization of benzofuropyridines by the action of activated alkynes in the synthesis of spiro[benzofuropyridines], representatives of a new class of acetylcholinesterase inhibitors. Chem. Heterocycl. Compd. 49 (2013) 930-940.

[45] M. de Candia, G. Zaetta, N. Denora, D. Tricarico, M. Majellaro, S. Cellamare, C.D. Altomare, New azepino[4,3-*b*]indole derivatives as nanomolar selective inhibitors of human butyrylcholinesterase showing protective effects against NMDA-induced neurotoxicity, Eur J Med Chem. 125 (2017) 288-298.

[46] L.G. Voskressensky, S.V. Akbulatov, T.N. Borisova, A.V. Kleimenov, A.V. Varlamov, Synthesis of hexahydroazonino[5,6-*b*]indoles from hexahydroazepino[4,3-*b*]- and-[3,4-*b*]indoles and activated alkynes, Russ. Chem. Bull. 56 (2007) 2323-2329.

[47] L.G. Voskressensky, S.V. Akbulatov, T.N. Borisova, A.V. Varlamov, A novel synthesis of hexahydroazoninoindoles using activated alkynes in an azepine ring expansion, Tetrahedron 62 (2006) 12392-12397.

[48] A.V. Ivachtchenko, E.B. Frolov, O.D. Mitkin, S.E. Tkachenko, A. Khvat, Synthesis and biological evaluation of novel bioisosteric analogues of Dimebon, Lett. Drug Des. Discov. 7 (2010) 446-451.

[49] G. L. Ellman, K. D. Courtney, V. Andres, R. M. Feather-Stone, A new and rapid colorimetric determination of acetylcholinesterase activity. Biochem. Pharmacol. 7 (1961) 88-95.

[50] Pisani, L.; Catto, M.,; De Palma, A.; Farina, R.; Cellamare, S.; Altomare, C. D. Discovery of potent dual binding site acetylcholinesterase inhibitors via homo- and heterodimerization of coumarin-based moieties. ChemMedChem 2017, 12 (16), 1349–1358.

[51] Pisani, L.; De Palma , A.; Giangregorio , N.; Miniero , D. V.; Pesce , P.; Nicolotti , O.; Campagna , F.; Altomare , C. D.; Catto, M. mannich base approach to 5-methoxyisatin 3-(4-isopropylphenyl)hydrazone: a water-soluble prodrug for a multitarget inhibition of cholinesterases, beta-amyloid fibrillization and oligomer-induced cytotoxicity. European Journal of Pharmaceutical Sciences 2017, 109, 381-388.

[52] M. Catto, R. Aliano, A. Carotti, S. Cellamare, F. Palluotto, R. Purgatorio, A. De Stradis, F. Campagna, Design, synthesis and biological evaluation of indane-2-arylhydrazinylmethylene-1,3-diones and indol-2-aryldiazenylmethylene-3-ones as beta-amyloid aggregation inhibitors. Eur. J. Med. Chem. 45 (2010) 1359-1366.

[53] F. Campagna, M. Catto, R. Purgatorio, C.D. Altomare, A. Carotti, A. De Stradis, G. Palazzo, Synthesis and biophysical evaluation of arylhydrazono-1*H*-2-indolinones as β-amyloid aggregation inhibitors. Eur. J. Med. Chem. 46 (2011) 275-284.

[54] L. Jalili-Baleh, H. Forootanfar, T.T. Küçükkılınç, H. Nadri, Z. Abdolahi, A. Ameri, M. Jafari, B. Ayazgok, M. Baeeri, M. Rahimifard, S.N.A. Bukhari, M. Abdollahi, M.R. Ganjali, S. Emami,

M. Khoobi, A. Foroumadi, Design, synthesis and evaluation of novel multi-target-directed ligands for treatment of Alzheimer's disease based on coumarin and lipoic acid scaffolds. Eur. J. Med. Chem. 152 (2018) 600-614.

[55] G.L.K. Hoh, D.O. Barlow, A.F. Chadwick, D.B. Lake, S.R. Sheeran, Hydrogen peroxide oxidation of tertiary amines. J. American Oil Chem. Soc. 40 (1963) 268-271.

[56] W.R. Wilson, W.A. Denny, S.M. Pullen, K.M. Thompson, A.E. Li, L.H. Patterson, H.H. Lee, Tertiary amine N-oxides as bioreductive drugs: DACA N-oxide, nitracrine N-oxide and AQ4N, Br. J. Cancer 74 Suppl. XXVII (1996), S43-S47.

[57] B.D. Belviso, R. Caliandro, M. de Candia, G. Zaetta, G. Lopopolo, F. Incampo, M. Colucci, C.D. Altomare, How a β-D-glucoside side chain enhances binding affinity to thrombin of inhibitors bearing 2-chlorothiophene as P1 moiety: crystallography, fragment deconstruction study, and evaluation of antithrombotic properties, J. Med. Chem. 57 (2014) 8563-75.

[58] M. de Candia, E. Marini, G. Zaetta, S. Cellamare, A. Di Stilo, C.D. Altomare, New organic nitrate-containing benzyloxy isonipecotanilide derivatives with vasodilatory and anti-platelet activity. Eur. J. Pharm. Sci. 72 (2015) 69-80.

[59] F. Cheng, W. Li, Y. Zhou, J. Shen, Z. Wu, G. Liu, P.W. Lee, Y. Tang, AdmetSAR: a comprehensive source and free tool for assessment of chemical ADMET properties. J. Chem. Inf. Model. 52 (2012) 3099-3105.

[60] D.E. Clark, Rapid calculation of polar molecular surface area and its application to the prediction of transport phenomena. 2. Prediction of blood-brain barrier penetration, J. Pharm. Sci. 88 (1999) 815-21.

[61] C.A. Lipinski, F. Lombardo, B. W. Dominy, P. J. Freeney, Experimental and computational approaches to estimate solubility and permeability in drug discovery and development settings, Adv. Drug Delivery Rev. 23 (1997) 3-25.

[62] H. Yang, L. Sun, Z. Wang, W. Li, G. Liu, Y. Tang, ADMETopt: A Web Server for ADMET Optimization in Drug Design via Scaffold Hopping, J. Chem. Inf. Model. 58 (2018) 2051-2056.

[63] D. Knez, N. Coquelle, A. Pišlar, S. Žakelj, M. Jukič, M. Sova, J. Mravljak, F. Nachon, X. Brazzolotto, J. Kos, J.P. Colletier, S. Gobec, Multi-target-directed ligands for treating Alzheimer's disease: Butyrylcholinesterase inhibitors displaying antioxidant and neuroprotective activities, Eur. J. Med. Chem. 156 (2018) 598-617.

[64] W.D. Cornell, P. Cieplak, C.I. Bayly, I R. Gould, K.M. Merz, D.M. Ferguson, D.C. Spellmeyer, T. Fox, J.W. Caldwell, P.A. Kollman, A Second Generation Force Field for the Simulation of Proteins, Nucleic Acids, and Organic Molecules, J. Am. Chem. Soc. 117 (1995) 5179-5193.

[65] G.M. Morris, D.S. Goodsell, R.S. Halliday, R. Huey, W.E. Hart, R.K. Belew, A.J. Olson, Automated Docking using a Lamarckian genetic algorithm and empirical binding free energy function, J. Comput. Chem. 19 (1998) 1639-1662.

[66] S. Forli, A. J. Olson, A Force Field with Discrete Displaceable Waters and Desolvation Entropy for Hydrated Ligand Docking J. Med. Chem. 55 (2012) 623-638.

[67] K.J. Bowers, E. Chow, H. Xu, R.O. Dror, M.P. Eastwood, B.A. Gregersen, J.L. Klepeis, I. Kolossvary, M.A. Moraes, F.D. Sacerdoti, J.K. Salmon, Y. Shan, D.E. Shaw, Scalable Algorithms for Molecular Dynamics Simulations on Commodity Clusters,Proceedings of the ACM/IEEE Conference on Supercomputing (SC06), Tampa, Florida, 2006, November 11-17.

Supplementary Material - For Publication Online

Click here to download Supplementary Material - For Publication Online: EJMECH-D-19-00581 - Revised Supp. Infos.docx